Design, Fabrication, and Performance of a Gas-Turbine Engine from an Automobile Turbocharger

by

Jorge Padilla, Jr.

SUBMITTED TO THE DEPARTMENT OF MECHANICAL ENGINEERING IN PARTIAL FULFILLMENT OF THE REQUIREMENT FOR THE DEGREE OF

BACHELOR OF SCIENCE IN MECHANICAL ENGINEERING
AT THE
MASSACHUSETTS INSTITUTE OF TECHNOLOGY

JUNE 2005

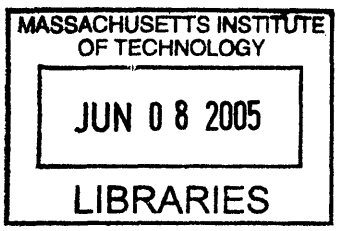

Signature of Author: _____
Department of Mechanical Engineering
May 23, 2005

Certified by: _____
Professor Ernest G. Cravalho
Professor of Mechanical Engineering
Thesis Supervisor

Accepted by: _____
Professor Ernest G. Cravalho
Chairman, Undergraduate Thesis Committee
Department of Mechanical Engineering

Design, Fabrication, and Performance of a Gas-Turbine Engine from an Automobile Turbocharger

by

Jorge Padilla, Jr.

Submitted to the Department of Mechanical Engineering
on May 23, 2005, in Partial Fulfillment of the
Requirements for the Degree of Bachelor of Science in
Mechanical Engineering

ABSTRACT

Thermal-Fluids Engineering is taught in two semesters in the Department of Mechanical Engineering at the Massachusetts Institute of Technology. To emphasize the course material, running experiments of thermodynamic plants are integrated into the course as demonstrations. The aim of this thesis is to supplement the course demonstrations of thermodynamic plants through the design and fabrication of a gas-turbine engine. The engine operates on an open version of the Brayton cycle. Students will be able to evaluate the energy conversion efficiency and net work ratio from air temperature measurements in three stages of the cycle.

The gas-turbine engine is made from an automobile turbocharger for its common shaft turbine and compressor. A combustion chamber was placed between the outlet of the compressor and the inlet of the turbine. The temperature measurement system was designed from the placement of thermocouples on the outside wall of a pipe leading from the compressor to the combustor, on the outside wall of a pipe leading from the combustor to the turbine, and on the outside wall of the turbine exhaust pipe. As the temperature measured by the thermocouple will be that of the outside walls of the engine, the model will depict the cross-sectional temperature profile so the students will know the actual bulk temperature of the working fluid, air.

Thesis Supervisor: Ernest G. Cravalho
Title: Professor of Mechanical Engineering

Table of Contents

CONTENTS

List of Figures

1. Introduction

Thermal-Fluids Engineering is taught in two semesters in the Department of Mechanical Engineering at the Massachusetts Institute of Technology. The curriculum consists of fundamental thermodynamics, fluid mechanics, and heat transfer as it applies to the design and analysis of thermal-fluids engineering systems. In the second semester of Thermal-Fluids Engineering, subject material focuses on the design of thermodynamic plants from the study of thermodynamics and fluid mechanics of steady flow components in these plants. To emphasize the course material, running experiments of thermodynamic plants are integrated into the course as demonstrations. The aim of this thesis is to supplement the course demonstrations of thermodynamic plants through the design and fabrication of a gas-turbine engine.

The gas-turbine engine is a useful enrichment apparatus because it operates on an open version of the Brayton cycle taught in the course. Furthermore, the engine includes components commonly found in engineering practice. The gas-turbine engine includes a compressor, a constant pressure heat exchanger, and a turbine. Finally, the gas-turbine engine is designed so that students are able to measure the steady-state temperature of the engine in each of the stages of the cycle. In this way, students can determine the energy conversion efficiency and net work ratio of the cycle.

The gas-turbine engine had to be designed suitably for a student demonstration such that it was mobile and operated at a safe maximum temperature. To fulfill the first requirement, the engine was built from an automobile turbocharger on a movable cart. An automobile turbocharger was selected for its common shaft compressor and turbine. To fulfill the second design requirement, propane was selected as the fuel due to its accessibility and its heating value. The constant pressure heat exchanger is manifested in a combustion chamber placed between the compressor outlet and the turbine inlet. In addition, a turbocharger cooling and lubrication system was designed that uses oil as the working fluid to cool the turbine and compressor shaft as well as to provide hydrodynamic bearings for the shaft. The ignition system was designed from a gas barbecue grill igniter. Finally, the temperature measurement system was designed from the placement of thermocouples on the outside wall of a pipe leading from the compressor to the combustor, on the outside wall of a pipe leading from the combustor to the turbine, and on the outside wall of the turbine exhaust pipe. A model for determining the mean bulk temperature of the working fluid, air, was developed from principles of convective and conductive heat transfer as well as turbulent fluid flow mechanics.

This thesis is the continuation of a project begun by Keane Nishimoto to fulfill his undergraduate thesis requirement [1]. The project was continued by Lauren Tsai in her fulfillment of the same requirement [2]. Nishimoto selected and purchased the automobile turbocharger and cooling and lubrication system components. Tsai designed the combustion chamber from Nishimoto's idea for a concentric shell design for combustion chambers.

The thesis begins with a background on gas-turbine power plants and the application of the laws of thermodynamics to determine the energy conversion efficiency and net work ratio. Next, a brief engine synopsis is given that introduces the individual engine components and their specifications. The engine synopsis is followed by several sections regarding the design of the combustion chamber and ignition system. A section on the design of the cooling and lubrication system follows the combustion section. The bulk of this document is dedicated thereafter to the development of the temperature profile model for determining the bulk mean air temperature in three different stages of the Brayton cycle. The thesis conclude with a conclusion and future recommendations for improving this project.

2. Gas Turbine Power Plants

Gas turbine power plants are thermodynamic systems that use fuel and air to produce a positive work transfer. The gas turbine plant runs on an open cycle with only one fluid circuit. The components of a gas turbine engine include a compressor, a combustion chamber, and a turbine assembled in series as shown in Figure 1.

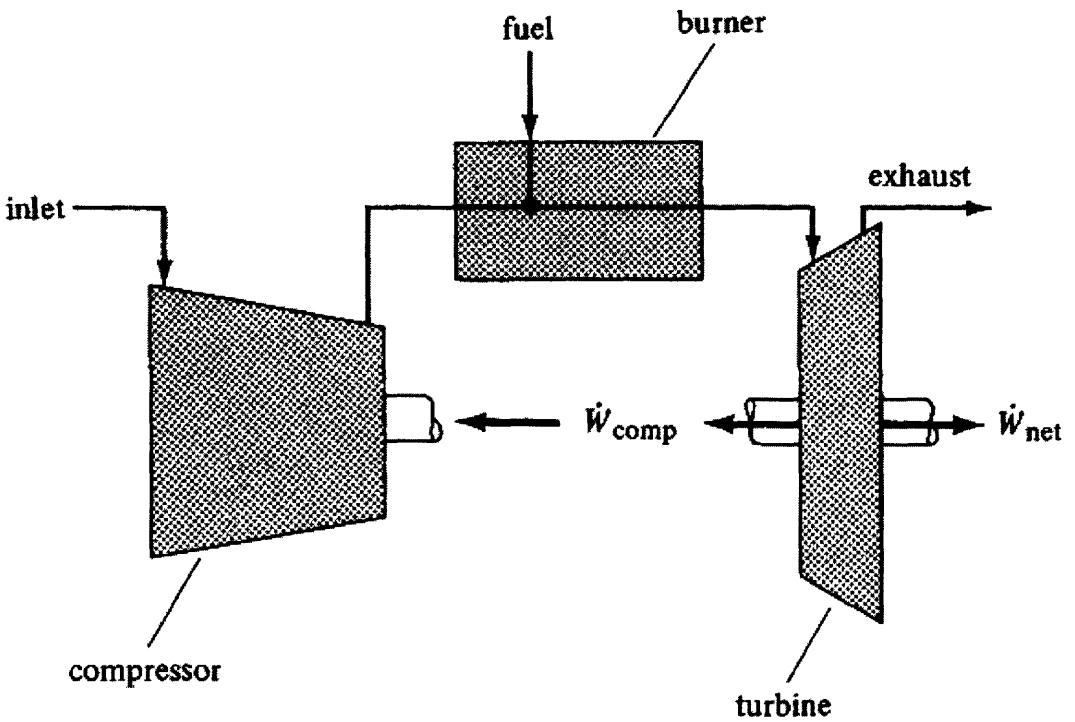

Figure 1: Components of a typical gas turbine plant [3]

The cycle begins when atmospheric air is drawn into the compressor and compressed by a negative work transfer, thereby, increasing both the pressure and temperature of the air. Next, the air, in its second state, enters the combustion chamber where its temperature and specific volume are increased by an isobaric heat transfer manifested in the combustion of fuel in the chamber. The heated air is then expanded in the turbine and exhausted to the atmosphere. The expansion of the air produces a positive work transfer because more work is produced in the expansion of the air at a high specific volume than the work required to compress the cold air entering the cycle at a lower specific volume.

It is desirable to simplify the model of the gas turbine plant to apply the closed cycle model for the plant, called the Brayton cycle. To apply the Brayton cycle, it must be assumed that the addition rate of fuel introduced in the combustion chamber is negligible compared to the mass flow rate of air through the engine. Furthermore, the combustion chamber is assumed to be a constant pressure heat exchanger. Finally, the heat transfer rate to the air is the product of the air mass flow rate and the heating value of the fuel.

The Brayton cycle consists of two adiabatic work transfers and two isobaric heat transfers. It is convenient to apply the Brayton cycle to the gas turbine plant because it illustrates the importance of the turbine inlet temperature, the compressor pressure ratio, and the compressor and turbine efficiencies on the overall performance of the engine. The Brayton cycle is depicted graphically in Figure 2. Note that the numbered points on the plot represent the state of air at each step of the cycle.

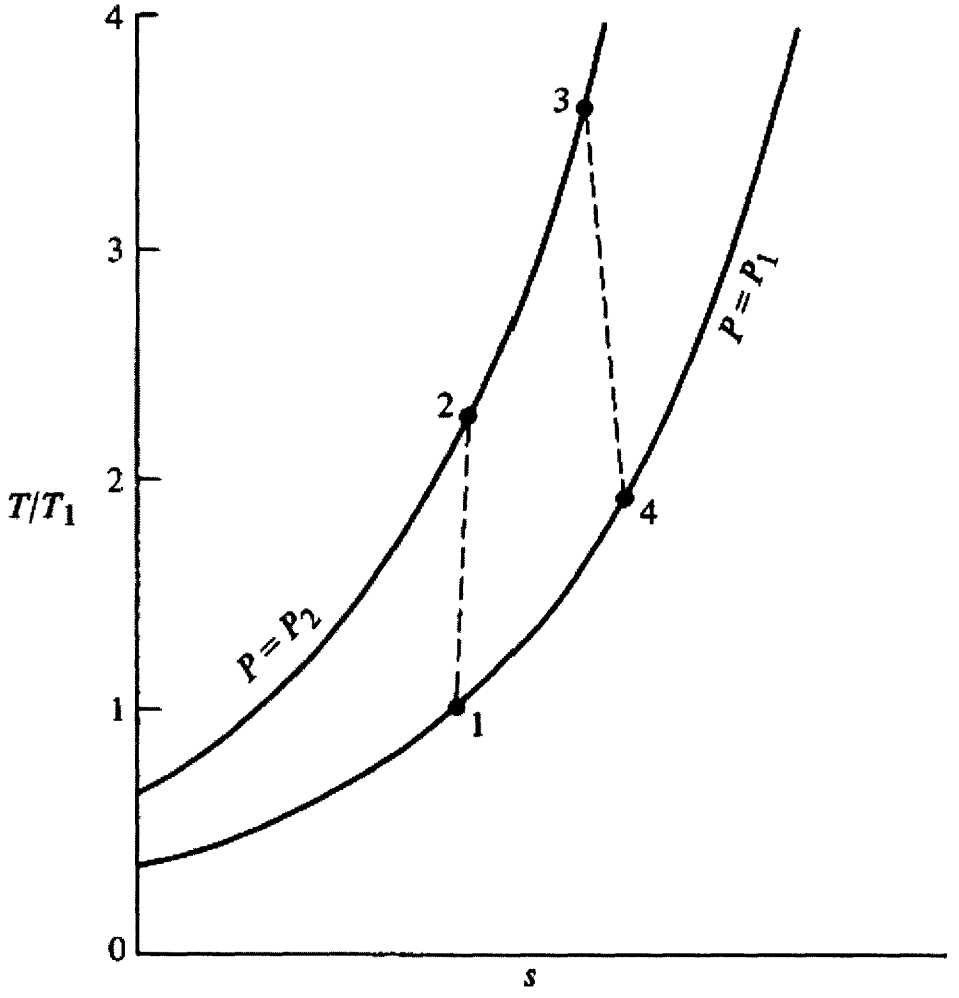

Figure 2: Graphical representation of Brayton cycle model for a gas turbine plant [3].

2.1 Application of the First Law to the Brayton Cycle

To apply the First Law of Thermodynamics to the gas turbine plant, the control volume is defined as shown in Figure 2.

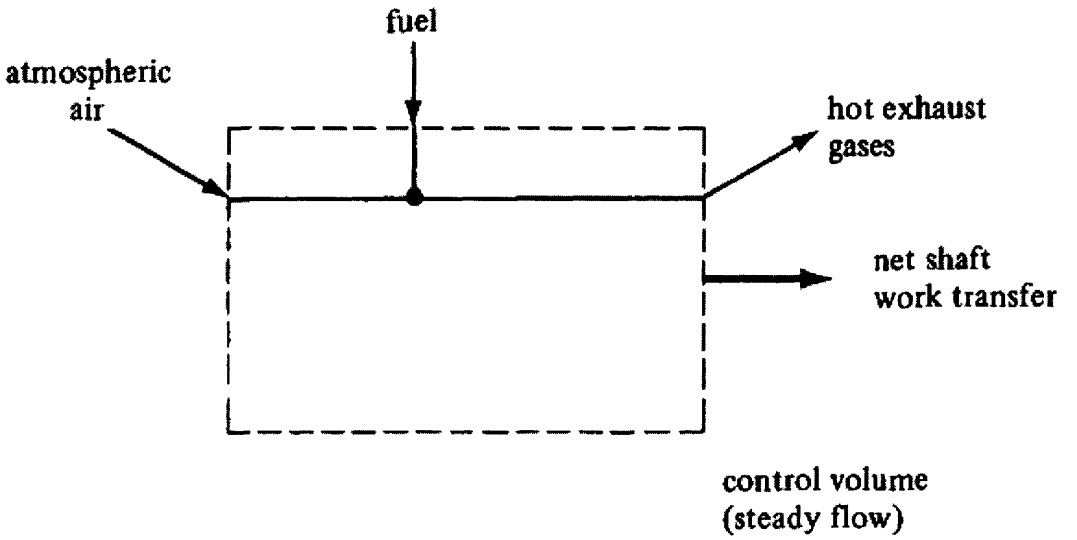

Figure 3: Schematic diagram of control volume for open cycle gas turbine plant [3].

For an open cycle, the first law of thermodynamics is given by,

$$\frac{dE_{CV}}{dt} = \dot{Q} - \dot{W}_{shaft} + \sum_{in} \dot{m}\left(h + \frac{u^2}{2} + gz\right) - \sum_{out} \dot{m}\left(h + \frac{u^2}{2} + gz\right), \qquad (1)$$

where $\frac{dE_{CV}}{dt}$ represents the rate of change of energy in the control volume with respect to time, $\dot{Q}$ is the heating rate of the control volume, $\dot{W}_{shaft}$ represents the work done on the control volume, $\dot{m}$ is the air mass flow rate, h is the enthalpy, u is the air velocity, g is the acceleration due to gravity, and z refers to position on the vertical, z-axis. Since the performance of the gas-turbine engine will be evaluated in the steady state, the total energy of the plant will be constant. Furthermore, the kinetic energy of and gravitational effects on the flow are insignificant when compared to the enthalpy of the flow. Therefore, the first law for this control volume in which mass is conserved is given by,

$$0 = \dot{Q} - \dot{W}_{shaft} + \dot{m}(h_{in} - h_{out}). \qquad (2)$$

To evaluate the performance of the Brayton cycle model for the gas turbine plant, it is useful to apply equation (2) for every step of the cycle. In the first cycle process, the air is compressed adiabatically and thus, the first law for the compressor power becomes,

$$\dot{W}_{\text{compressor}} = \dot{m}(h_1 - h_2) = \dot{m}C_P(T_1 - T_2), \tag{3}$$

where, C_P is the specific heat of air. In this problem, C_P is assumed to remain constant. Next, heat is added to the air at constant pressure in the combustion chamber. Since there is no change in pressure, there is no work done on the air. The first law for this process is given by,

$$\dot{Q}_{\text{added}} = \dot{m}(h_3 - h_2) = \dot{m}C_P(T_3 - T_2). \tag{4}$$

In the third process, the air is expanded adiabatically in the turbine. The first law for this process is shown by,

$$\dot{W}_{\text{turbine}} = \dot{m}(h_3 - h_4) = \dot{m}C_P(T_3 - T_4). \tag{5}$$

In the fourth process, heat is rejected to a heat exchanger to return the air to its initial state. The first law for this process is,

$$\dot{Q}_{\text{rejected}} = \dot{m}(h_1 - h_4) = \dot{m}C_P(T_1 - T_4). \tag{6}$$

In this experiment, the environment represents the heat exchanger in the final process of the cycle. The heat transfer is accomplished by exhausting the hot air to the atmosphere.

2.2 Application of the Second Law to Determine Compressor Efficiency

As it is manifested in equation (3), compressors increase the temperature and pressure of a working fluid through negative shaft work. The compression of the fluid is considered to be an adiabatic process because often the working fluid does not reside in the compressor long enough to allow significant heat transfer. If it is assumed that the fluid compression is done so reversibly, the second law of thermodynamics for the compressor is given by,

$$s_2 - s_1 = C_P \ln\frac{T_2}{T_1} - R\ln\frac{P_2}{P_1} = 0. \tag{7}$$

If the initial temperature and pressure ratio of the compressor are known, it is possible to predict the reversible air temperature, T_{2R} of the compressed air from equation (7) as shown by,

$$T_{2R} = T_1\left(\frac{P_2}{P_1}\right)^{\frac{\gamma-1}{\gamma}}, \tag{8}$$

where γ is given by,

$$\gamma = \frac{C_p}{C_v}. \tag{9}$$

In equation (9), C_p is the air specific heat at constant pressure and C_v is the air specific heat at constant volume. γ for air is 1.4.

The compressor efficiency η_C is determined from the ratio of work required to compress the air reversibly to the work required to compress the air irreversibly. The reversible work transfer is found by substituting the reversible air temperature determined in equation (8) into equation (3) such that,

$$\dot{W}_{\text{reversible}} = \dot{m} C_P (T_1 - T_{2R}). \tag{10}$$

Therefore, the compressor efficiency is given by,

$$\eta_C = \frac{\dot{W}_{\text{reversible}}}{\dot{W}_{\text{irreversible}}} = \frac{(T_1 - T_{2R})}{(T_1 - T_2)}. \tag{11}$$

2.3 Application of the Second Law to Determine Turbine Efficiency

Turbines decrease the temperature and pressure of a working fluid through positive shaft work. If the air in the turbine is assumed to be expanded adiabatically and isentropically, due to its insufficient residence time for heat transfer, the reversible exhaust temperature, T_{4R}, is found from the second law by

$$T_{4R} = T_3 \left(\frac{P_4}{P_3} \right)^{\frac{\gamma - 1}{\gamma}}. \tag{12}$$

The turbine efficiency η_T is determined from the actual, positive work done during the air expansion to the reversible work done and is given by

$$\eta_T = \frac{\dot{W}_{\text{actual}}}{\dot{W}_{\text{reversible}}} = \frac{(T_4 - T_3)}{(T_{4R} - T_3)}. \tag{13}$$

2.4 Application of First Law to the Combustion Chamber

The first constant pressure heat transfer for this Brayton cycle occurs in the combustion chamber. The compressed air enters the combustion chamber and heat is transferred to it as a result of the combustion process that converts the chemical potential energy fuel to thermal energy. The heat transfer is manifested in the increase in temperature and specific volume air. As there is no work done on the air in this stage of the Brayton cycle, the first law is given by equation (4). However, it is useful to apply

the first law in terms of the reactants and products of the combustion process as shown by,

$$\dot{Q} = \sum_{\text{in}} \left(\dot{n}\bar{h}\right) - \sum_{\text{out}} \left(\dot{n}\bar{h}\right), \tag{14}$$

where $\dot{n}$ is the flow rate of the individual reactants and products measured in mols per second.

The individual enthalpies for the products and reactants are calculated from the sum of the enthalpy of formation, $\bar{h}^{o}_{T,P}$, at standard temperature, 25 C, and pressure, 1 atmosphere, and the enthalpy required to raise the products and reactants from standard temperature and pressure (STP). The resulting enthalpy is given by,

$$\bar{h} = \bar{h}^{o}_{T,P} + \left(\bar{h}_{T,P} - \bar{h}_{STP}\right). \tag{15}$$

In the combustion process, stoichiometric air is mixed with propane and burned to yield carbon-dioxide and water as depicted by the reaction

$$C_3H_8 + 5O_2 + 5(3.76)N_2 \rightarrow 3CO_2 + 4H_2O + 5(3.76)N_2 . \tag{16}$$

Nitrogen does not react in the reaction, but is present in the combustion chamber.

2.5 Brayton Cycle Efficiency

Having determined the heat transfer and the work done it is possible to evaluate the energy conversion efficiency, η_{cycle}, and the work ratio, NWR. η_{cycle} is found from the ratio of the net work, $\dot{W}_{\text{net}}$, to the heat transfer in the combustion chamber as shown by

$$\eta_{\text{cycle}} = \frac{\dot{W}_{\text{net}}}{\dot{Q}_{2\text{-}3}} = 1 - \frac{T_4 - T_3}{T_3 - T_2}. \tag{17}$$

The net work ratio is determined from the ratio of the net work to the heat transfer required to restore the air to its initial conditions as shown by

$$\text{NWR} = \frac{\dot{W}_{\text{net}}}{\dot{Q}_{3\text{-}4}} = 1 - \frac{T_2 - T_1}{T_3 - T_4} . \tag{18}$$

2.6 Engine Synopsis

The most critical design requirements of the engine were that its size, mobility, and accessibility be appropriate for classroom experimentation. These requirements are fulfilled by building the engine on a rolling cart that measures about 90 cm in length, 60 cm in width, and 60 cm in height.

An automobile turbocharger was selected for its common shaft compressor and turbine. The details of the automobile turbocharger will be delineated in the next section. The turbocharger was placed on the top shelf of the cart and oriented such that air enters the compressor horizontally. Next, the air is directed vertically upwards from the compressor to the combustion chamber by a welded J-pipe. Fuel is fed through the top of the combustion chamber from a fuel tank located on the bottom shelf of the cart. The working fuel in this project is propane and supplied at an appropriate rate to achieve an adequate maximum cycle temperature. The air is exhausted from the combustion chamber to the turbine inlet by a vertical pipe. Finally, the turbine is oriented so that air exhausts horizontally. However, as will be shown in section 4.1, the exhaust temperature of air will be on the order of 700 K and so it was necessary to direct the exhaust vertically upwards for safety reasons. The air is directed upwards by an automobile exhaust pipe with a 90^{o} turn. The turbocharger uses oil as a hydrodynamic bearing for the shaft as well as a coolant. The oil is pumped from a reservoir, which is also located on the bottom shelf of the cart.

2.7 Engine Turbocharger

The turbocharger selected for this project is a model K26 manufactured by Kühnle, Kopp, & Kausch (3K), a division of Borg Warner Turbo Systems. The turbocharger was removed from a 1985 Audi 200 5T automobile. Keane Nishimoto purchased the turbocharger in good condition from an auto salvage dealership [1]. It was important to select a turbocharger whose compressor and turbine housing and blades had been well-preserved because the efficiency of the engine greatly depends on the efficiency of the compressor and turbine.

The turbocharger works much the same on the gas turbine as it does on an automobile. In an automobile, the compressor compresses air from the intake manifold flowing to the engine cylinders. After the fuel and compressed air are burned in the cylinders, the air is exhausted to the turbine where it passes over the turbine blades that cause the shaft to spin [12]. Since the turbine and the compressor reside on the same shaft, the compressor blades are spun, compressing more air. In this project, the engine cylinders are replaced by the combustion chamber.

The performance characteristics for the compressor of the K26 turbocharger are represented in the performance map provided by Borg Warner Turbo Systems and shown in Figure 4. The performance characteristics for the turbine are represented in the performance map shown in Figure 5.

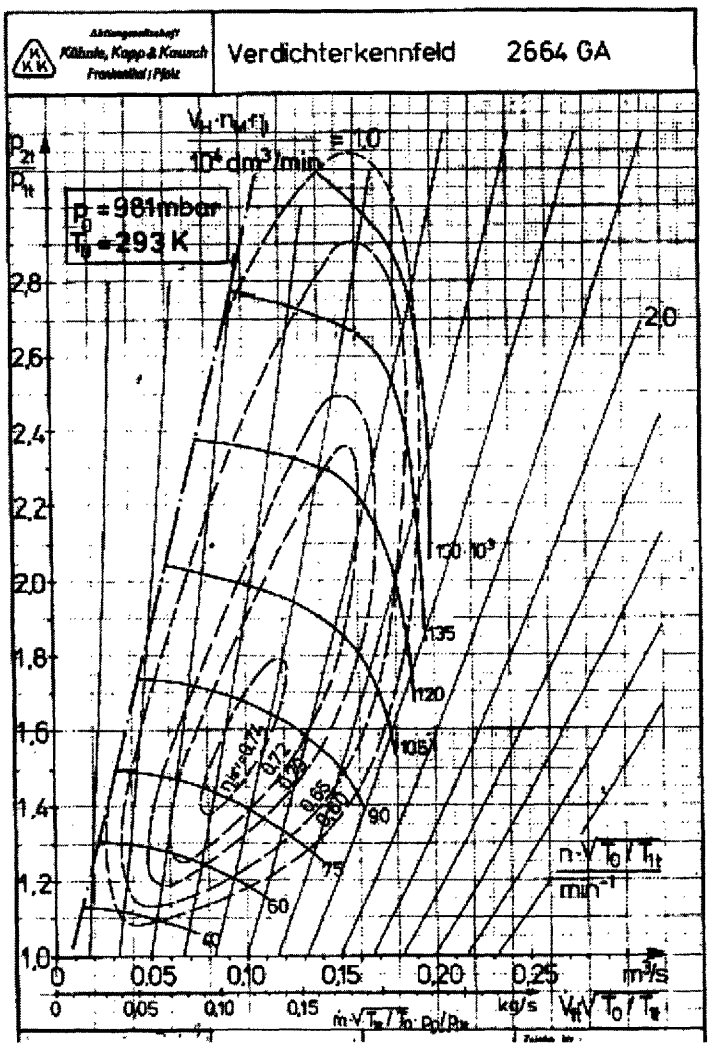

Figure 4: Compressor map [2].

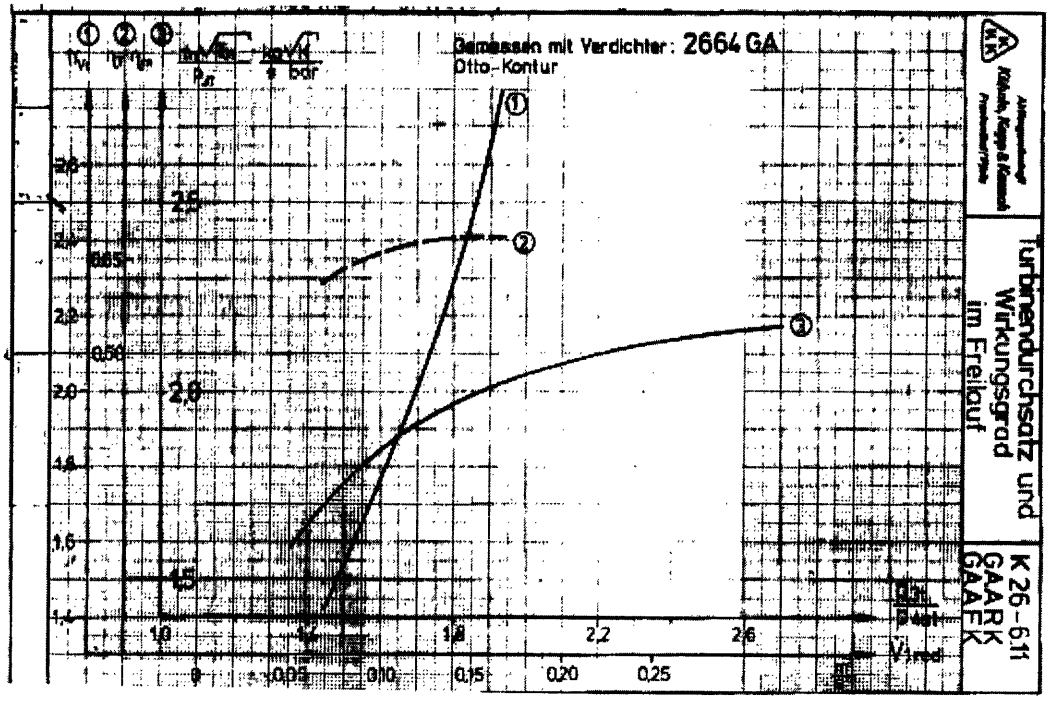

Figure 5: Turbine map [2].

3. Combustion Chamber Design

The combustion chamber was designed by Lauren Tsai [2]. The design was inspired by the design of other gas turbine engines that had been fabricated from turbochargers. The combustion chamber was designed to self-sustain a flame for continuous ignition and to exhaust combustion products at a suitable working temperature for the turbine. If the exhaust temperature exceeds a maximum working temperature of the turbine, the turbine housing and blades could be damaged.

Although all combustor designs vary, all combustion chambers have three features: (1) a recirculation zone, (2) a burning zone (with a recirculation zone which extends to the dilution region), and (3) a dilution zone [4]. In the recirculation zone, the fuel is evaporated and partly burned in preparation for rapid combustion within the remainder of the burning zone. In an ideal combustion chamber, all of the fuel is combusted and is mixed with dilution air to cool it before it is exhausted to the turbine. However, if the fuel has not been completely combusted, chilling can occur, preventing completion of the combustion process. On the other hand, if the burning zone is run exceedingly rich, combustion can occur in the dilution zone.

The combustion chamber designed by Tsai includes the three features in the two areas: the primary zone and the secondary zone as depicted by Figure 6.

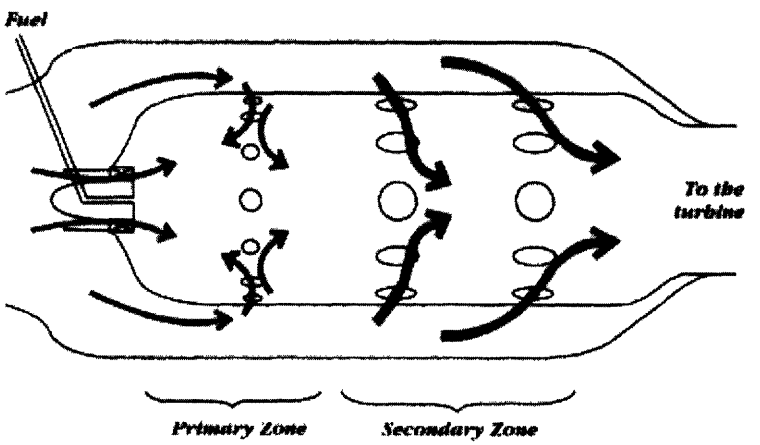

Figure 6: Combustion zones in combustor [2].

In the presence of a stoichiometric mixture of fuel and air, the greater part of the combustion process occurs in the primary zone. In the secondary zone, dilution air is mixed with combustion products to cool the mixture before it enters the turbine [Tsai, 17]. The combustion chamber was designed from a concentric tube model used in other similar projects as depicted in Figure 7.

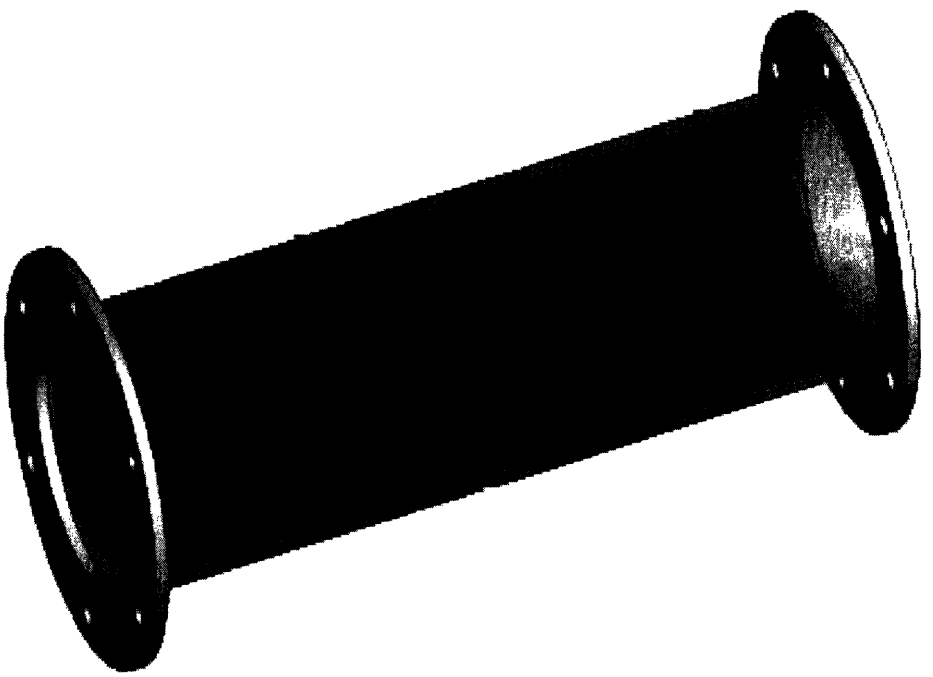

Figure 7: Concentric tube design [2].

In Figure 7, the inner, shaded shell represents the flame tube and is made from 22-gauge perforated steel. The outer shell is a 10.16 cm (4") inner diameter steel pipe. In operation, compressed air from the compressor enters the combustion chamber and flows through and around the flame tube. The air is burned with the fuel in the flame tube and the air that flows on the outside of the tube cools the products of combustion. It is important to control the mass flow rate of air into and around the flame tube because the fuel mass to air mass ratio in the flame tube will determine the sustainability of the flame. A low fuel to air ratio would indicate that the engine is running lean whereas the converse indicates that the engine is running rich. In the next section, a method will be developed to determine the appropriate air to fuel ratio required to sustain a stable flame in the combustor.

4. The Combustion Reaction

4.1 Estimating Operating Temperatures

The analysis begins by estimating the mass flow rate of air entering the combustion chamber from the compressor. From the Borg Warner compressor performance map it is possible to calculate a corrected mass flow rate. The corrected mass flow rate is calculated by,

$$\dot{m}\sqrt{\frac{T_1}{T_0}}\frac{P_0}{P_1} = 0.125\frac{\text{kg}}{\text{sec}} \quad , \tag{19}$$

$$\frac{P_2}{P_1} = 2 \quad , \tag{20}$$

and

$$\eta_C = 0.72 \quad . \tag{21}$$

$P_1 = 10^5 \text{N/m}^2$ is the initial pressure of air entering the compressor and $T_1 = 298\text{K}$ is the initial air temperature. The mass flow rate of air, in mols per second, in the compressor is calculated from equation (19) to yield

$$\dot{m}_{\text{air}} = \left(0.125\frac{\text{kg}}{\text{sec}}\right)\left(7.283\frac{\text{molAir}}{\text{kg}}\right) = 0.910\frac{\text{molAir}}{\text{sec}} \quad . \tag{22}$$

From equations (8) it is possible to predict the reversible temperature of air entering the combustor as shown

$$T_{2R} = T_1\left(\frac{P_2}{P_1}\right)^{\frac{\gamma-1}{\gamma}} = 363.3\text{K} \, . \tag{23}$$

Next, the irreversible air temperature entering the combustor is calculated from the combination of equations (21) and (23) as shown by

$$\eta_C = \frac{(T_1 - T_{2R})}{(T_1 - T_2)} \Rightarrow T_2 = 388.6\text{K}. \tag{24}$$

To prevent damage to the turbine components from extreme air temperatures, a turbine exhaust temperature of 700 K is selected at a 1 to 2 pressure ratio and an efficiency, $\eta_T = 0.70$, from the turbine performance map. From this information and by combining equations (12) and (13) it is possible to determine the temperature of air after the combustion process. The temperature of the air after combustion is given by,

$$T_3 = \frac{T_4}{\eta_T\left[\left(\frac{P_4}{P_3}\right)^{\frac{\gamma-1}{\gamma}} - 1\right] + 1} = 800\text{K} \quad . \tag{25}$$

4.2 Determing Fuel Supply Rate

The mass flow rate of propane is determined from the combustion reaction shown by equation (16). This chemical reaction equation assumes that there is a stoichiometric ratio of air to propane in the combustion process. However, the concentric shell design does not permit all of the compressed air to enter the flame tube. If the $\dot{x}$ represents the molar flow rate of propane per second and $\dot{y}$ represents the molar flow rate of air per second, then equation (14) is given by

$$\dot{x}\bar{h}_{C_3H_8} + \dot{y}\bar{h}_{O_2} + 3.76\dot{y}\bar{h}_{N_2} = 3\dot{x}\bar{h}_{CO_2} + 4\dot{x}\bar{h}_{H_2O} + 3.76\dot{y}\bar{h}^*_{N_2} + (\dot{y} - 5\dot{x})\bar{h}^*_{O_2}. \tag{26}$$

The molar flow rate of propane from equation (26) is

$$\dot{x} = 0.028\frac{\text{mol}C_3H_8}{\text{sec}} \Rightarrow 0.001232\frac{\text{kg}}{\text{sec}}. \tag{27}$$

A stoichiometric balance of the air to propane yields the molar flow rate of air of

$$\dot{y} = 0.139\frac{\text{molAir}}{\text{sec}} \Rightarrow 0.019\frac{\text{kg}}{\text{sec}}. \tag{28}$$

Therefore, the burned air to total compressed air ratio is given by

$$\frac{\dot{m}_{\text{airburned}}}{\dot{m}_{\text{air}}} = 0.153, \tag{29}$$

which means that 15.3% of the air from the compressor should be burned in the flame tube [2].

Figure 8 illustrates the cross-section of the combustion chamber where the compressed air is forced through or around the flame tube. The air enters the flame tube by way of a hole in the center of a flow plate. The air that does not flow through the plate flows radially outward through the greater area. The area of the hole in the flow plate is 15.3% of the cylindrical surface area through which the unburned air flows. It is important to note the expansion of the hole in the flow plate through the thickness of the plate. The expansion reduces the speed of the air to prevent a pressure drop in the flame tube and to prevent the air from extinguishing the flame on the fuel hook. Furthermore, the expansion directs the air flow over the fuel hook. The fuel hook is the subject of the next section.

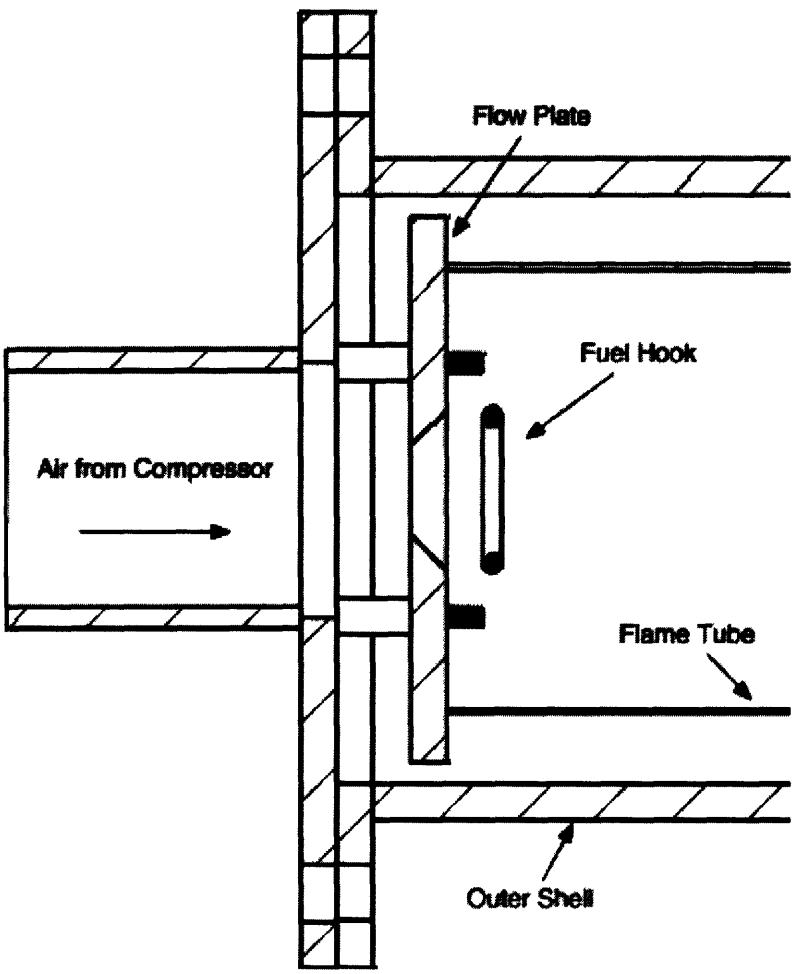

Figure 8: Cross-section of combustion chamber as air enters from the compressor [2].

4.3 Fuel Injection

The propane flow into the combustion chamber is regulated by a series of valves and a propane regulator. The propane regulator is affixed to the fuel tank outlet and is rated to a supply pressure of 4.1×10^5 Pa (60 psi). The regulator is a Turbo Torch Model R-LP Regulator used on propane torches. There is a pressure gauge shortly downstream of the regulator reads that the propane supply pressure. The propane is further regulated by a needle valve located downstream of the first pressure gauge. A second pressure gauge is placed beyond the needle valve used to measure the propane pressure at the outlet of the needle valve. Finally, the propane flows into the fuel hook located inside the combustion chamber.

The fuel hook is made from 3.175 mm (1/8") outer diameter, stainless steel tubing. The fuel hook is bent into a hook shape and six holes, 1.32 mm (0.052") in diameter are drilled along the average circumference of the hook. The end of the hook is welded shut. In operation, the propane is forced to flow out of the hook to burn small flames arranged in a circular pattern. The design is modeled after the design for the standard gas stove burner as well as a similar gas turbine built in the United Kingdom [5]. The fuel hook is pictured in Figure 9.

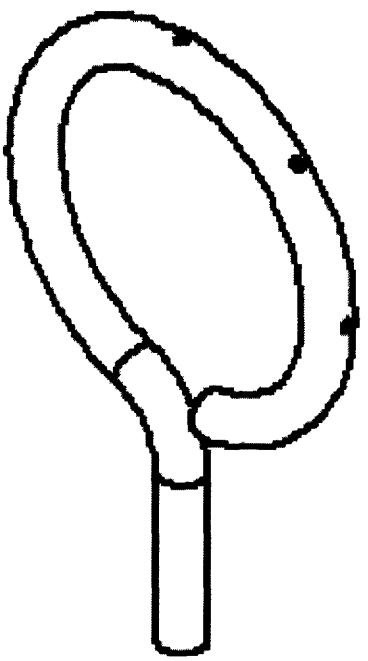

Figure 9: Fuel Hook [2].

The area of the holes in the fuel hook determines the pressure regulation at the propane regulator and the needle valve. The flow of the propane through the fuel hook can be treated as an orifice flow plate [2]. The volumetric flow rate, $\dot{V}_{\text{actual}}$, calculated from the propane mass flow rate, through an orifice is given by,

$$\dot{V}_{\text{actual}} = C_d A_t \sqrt{\frac{2(P_{\text{valve}} - P_2)}{\rho\left[1-\left(\frac{A_t}{A_1}\right)\right]}}. \tag{30}$$

P_2 is the pressure of the combustion chamber, expected to be 2×10^5Pa from equation (20), P_{valve} is the pressure of the propane flow at the outlet of the needle valve, A_t is the area of the fuel hook orifice, A_1 is the area at the fuel hook inlet, and C_d is the flow coefficient. Since the propane is supplied continuously from a reservoir, the area at the fuel hook inlet can be assumed to approach infinity. As a result, equation (30) is rewritten as

$$\dot{V}_{\text{actual}} = C_d A_t \sqrt{\frac{2(P_{\text{valve}} - P_2)}{\rho}}, \tag{31}$$

where the flow coefficient for this situation is $C_d = 0.5961$. Solving for the flow pressure at the needle valve yields,

$$P_{\text{valve}} = \left(\frac{\dot{V}_{\text{actual}}}{C_d A_t}\right)^2 \frac{\rho}{2} + P_2. \tag{32}$$

Next, the volumetric flow rate of propane through the valve, $\dot{V}_{\text{valve}}$, is calculated from,

$$\dot{V}_{\text{valve}} = C_{\text{v}} \sqrt{\frac{2(P_{\text{o}} - P_{\text{valve}})}{\gamma_{C_3H_8}}}, \tag{33}$$

where C_{v} is the flow coefficient of the valve, P_{o} is the flow pressure at the propane regulator, and $\gamma_{C_3H_8}$ is the specific gravity of propane. The value of the valve flow coefficient was found by Tsai to vary between 0.02 and 0.18 and thus, a valve with a maximum coefficient of 0.42 was selected for the engine. Finally, the pressure at the propane regulator was set such that

$$P_{\text{o}} = 206{,}842\text{Pa}, \tag{34}$$

$$P_{\text{valve}} = 200{,}003\text{Pa}, \tag{35}$$

with a flow coefficient of

$$C_v = 0.175. \quad (36)$$

4.4 Ignition System

The ignition system uses a push-button igniter from a Charbroil gas barbecue grill. The igniter has an internal piezoelectric crystal that generates a spark when the push-button is depressed. The push-button depression activates a spring loaded hammer that applies a pressure on the crystal inducing a great potential difference on the crystal [11]. The voltage is carried through the main burner extension wire to an electrode at the end of the wire. The electrode is passed through holes on the top of the combustion chamber and the flow plate. The electrode is electrically insulated from the steel wall by passing it through a ceramic cylinder [2]. The tip of the electrode is located 4.636 mm (0.1825") from one of the fuel hook holes. The combustion process is initiated when the push-button is depressed. The push-button igniter is pictured in Figure 10. The ignition system and combustion chamber inlet assembly are illustrated in Figure 11.

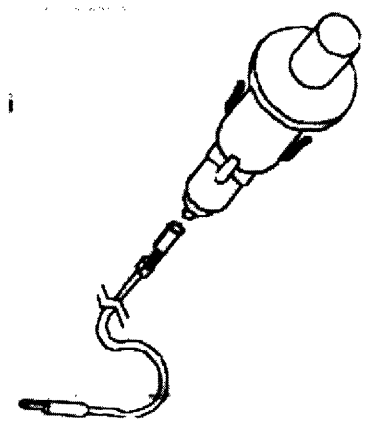

Figure 10: Push-button igniter assembly [2].

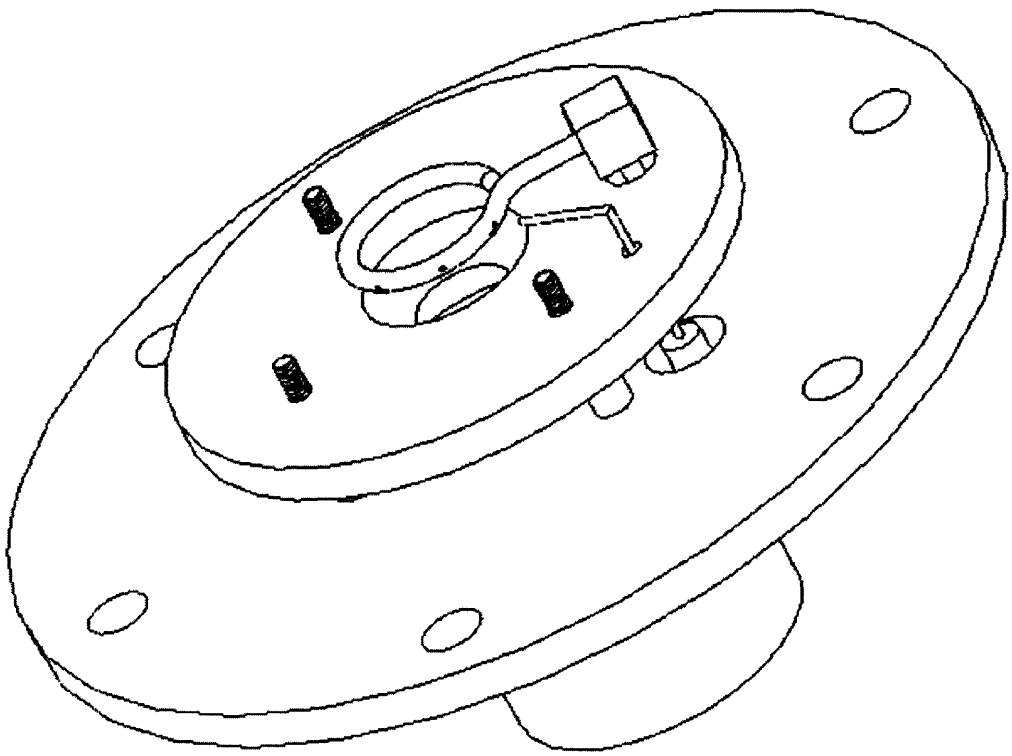

Figure 11: Ignition system and combustion chamber inlet [2].

5. Lubrication and Cooling System

5.1 System Components

The turbocharger requires oil for cooling during operation as well as for lubrication. The turbine and compressor shaft ride on the hydrodynamic bearings created by a thin film of oil. The hydrodynamic bearings make it possible for turbochargers to achieve angular speeds of 150,000 RPM.

The lubrication and cooling system developed in this project includes a 7.57 L (2 gallon) oil reservoir on the bottom shelf of the cart and a system of oil lines from the reservoir to the turbocharger returning to the reservoir. The oil is drawn from the reservoir by an oil pump and is next pumped through an oil filter before it reaches the turbocharger. The oil pump used for this engine is a Melling Model M-68, the same used on a Ford 302 truck engine. The oil pump is pictured in Figure 12. The oil filter is an Arrow Pneumatics 9.525 mm (0.375") inline Viton filter, model 9053V. Finally, the oil pressure was measured at the turbocharger inlet with an Ashcroft 38.1 mm (1.5") oil gauge, with a range of 0 to 413.7 kPa (60 psi).

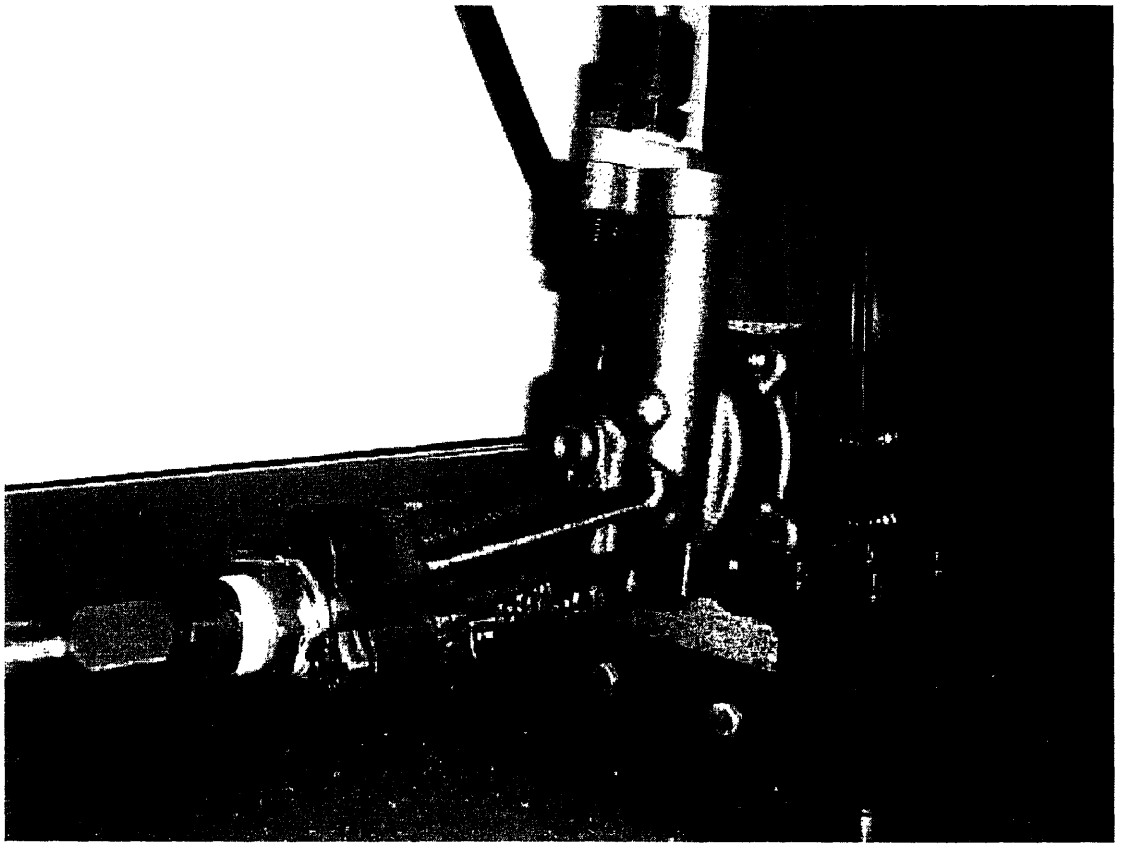

Figure 12: Melling Model M-68 Oil Pump [2]

5.2 Turbocharger Pumping Requirements

Borg Warner Turbo Systems specifications indicate that oil is pumped through the turbocharger at a mass flow rate, $\dot{m}_{oil}$ of

$$1.87\frac{\text{kg}}{\text{min}} \le \dot{m}_{oil} \le 2.49\frac{\text{kg}}{\text{min}} \quad . \tag{37}$$

The oil pressure specification requires that the oil be pumped a pressure, P_{oil} of

$$275.8\,\text{kPa} \le P_{oil} \le 344.7\,\text{kPa}\,, \tag{38}$$

with a lower limit of 241.3 kPa (35 psi) and an upper limit of 413.7 kPa (60 psi).

5.3 Pump Power Requirements

The Melling Model M-68 oil pump is a positive displacement pump. Positive displacement pumps deliver a definite volume of fluid per pumping cycle regardless of any flow restriction imposed upon it. This means that an in ideal pump, only the angular speed of operation determines the fluid mass pumping rate [6].

The first and second laws of thermodynamics can be applied to the pump to determine the work required to pump a definite volume of fluid with a flow restriction imposed upon the pump. The second law for pumping an incompressible fluid, steadily through a reversible and adiabatic pump is given by,

$$\dot{S}_{gen} = \dot{m}(s_{out} - s_{in}) = \dot{m}c\ln\frac{T_{out}}{T_{in}} = 0\,, \tag{39}$$

which means that $T_{out} = T_{in}$ and energy, E is conserved so that $E_{out} = E_{in}$. As a result, the first law is given by,

$$-\dot{W}_{shaft} = \dot{m}(h_{out} - h_{in}) = \dot{m}\left[(u_{out} - u_{in}) + \frac{P_{out} - P_{in}}{\rho}\right] = \rho\dot{V}_{oil}\left(\frac{P_{out} - P_{in}}{\rho}\right). \tag{40}$$

Melling Engine Parts pump specifications indicate that the Model M-68 is capable of pumping oil at a volumetric flow rate, $\dot{V}_{oil}$, of $2.77\times10^{-4}\,\frac{\text{m}^3}{\text{s}}$ at a shaft speed, ω_{shaft}, of $73.8\frac{\text{rad}}{\text{s}}$ or $705\frac{\text{rev}}{\text{min}}$ when no flow restriction is imposed on the pump. When a pump is operated with no flow restriction present the process is commonly referred to as freewheeling. This information is useful in determining the amount of work required to pump $\dot{V}_{oil}$ when a flow restriction is present. From equation (40), it is possible to

determine the amount of work required to pump oil at the freewheeling rate when the flow restriction from the gas-turbine engine is imposed upon the pump.

It is assumed that the oil pressure at the inlet of the pump is approximately atmospheric pressure. The hydrostatic pressure or head of the oil in the reservoir is negligible when compared to atmospheric pressure. The pressure of the oil at the outlet of the pump is the average pressure of the Borg Warner Turbo Systems specifications given by inequality (38). The density of oil is estimated at a value of $800\frac{\text{kg}}{\text{m}^3}$. Substituting these values into equation (40) gives,

$$-\dot{W}_{\text{shaft}} = \dot{V}_{\text{oil}}\left(P_{\text{out}} - P_{\text{in}}\right) = 58.3\ \text{W}. \tag{41}$$

The actual work required to pump the amount of oil specified by Borg Warner Turbo Systems is given by equation (40) such that

$$-\dot{W}_{\text{shaft, actual}} = \dot{V}_{\text{oil}}\left(P_{\text{out}} - P_{\text{in}}\right) = 9.5\ \text{W}. \tag{42}$$

The ratio of the work from equation (41) to the actual work from equation (42) results in a scaling factor useful for determining the actual shaft speed for the gas turbine. The scaling factor is given by,

$$X = \frac{\dot{W}_{\text{shaft}}}{\dot{W}_{\text{shaft, actual}}} = 6.114. \tag{43}$$

The actual shaft speed, $\omega_{\text{shaft, actual}}$ is then given by,

$$\omega_{\text{shaft, actual}} = \frac{\omega_{\text{shaft}}}{X} = 12.8\frac{\text{rad}}{\text{s}}. \tag{44}$$

The torque, τ required for operation is given by,

$$\tau = \frac{\dot{W}_{\text{shaft, actual}}}{\omega_{\text{shaft, actual}}} = 0.744\ \text{N}\cdot\text{m}. \tag{45}$$

5.4 Powering the Pump

A 14.4 V Milwaukee cordless power drill manufactured by Grainger, Inc. was selected to power the oil pump by a 6.35 mm (0.25") hex shaft. A saddle for the drill was constructed and placed on the bottom shelf of the cart. The drill was mounted upside down on the saddle as pictured in Figure 13.

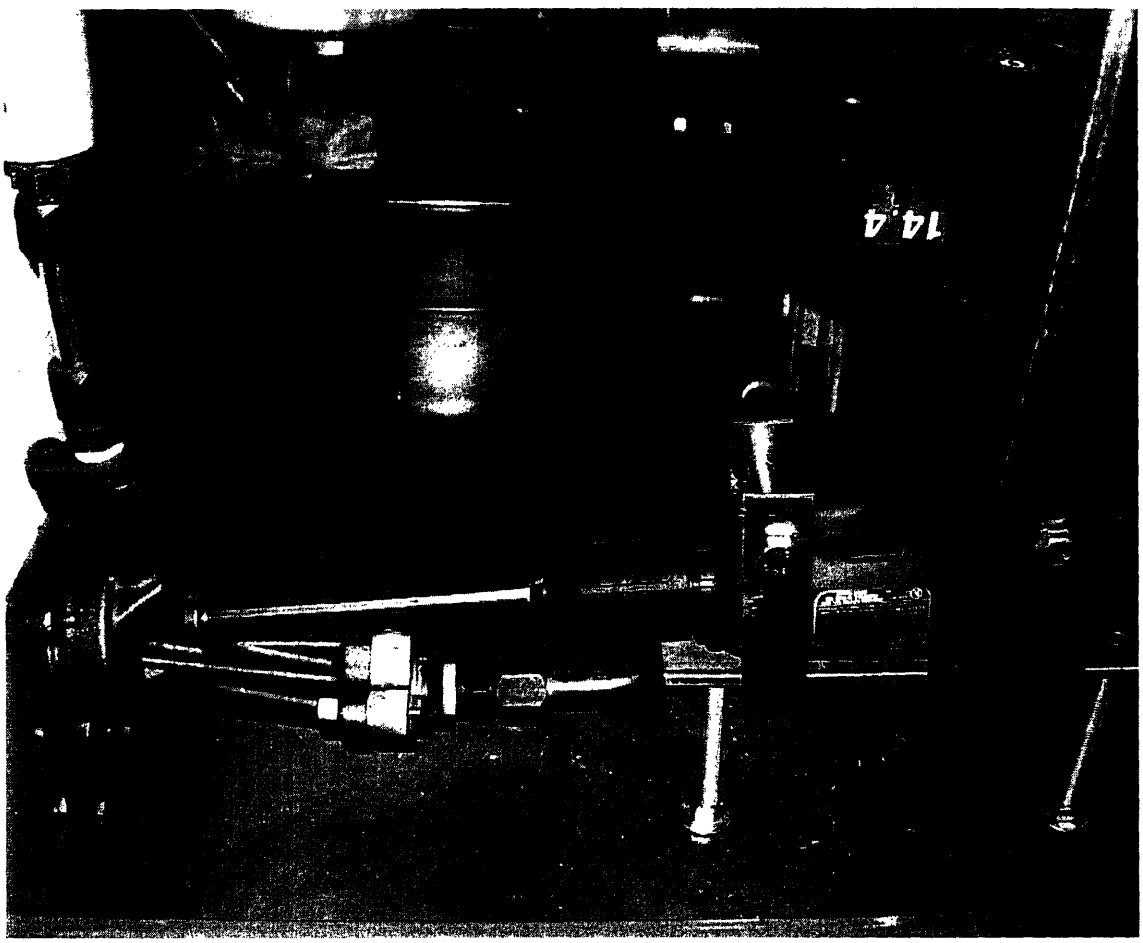

Figure 13: Cordless hand drill as power source for oil pump.

6. Bulk Mean Air Temperature

As shown in section 2.5, to determine the energy conversion efficiency and the net work ratio of the gas turbine engine, four temperatures are required. Of the desired temperatures, the first, T_1 is the bulk mean temperature of the working fluid, air in this case, as it enters the compressor. The second temperature, T_2 is the bulk mean air temperature measured between outlet of the compressor and the inlet to the combustor. The third temperature, T_3 is the bulk mean air temperature measured between the combustor outlet and the inlet to the turbine. Finally, the fourth temperature, T_4 is the bulk mean temperature of the air measured at the exhaust of the turbine.

To determine the bulk mean temperature of the air during the different stages of the Brayton cycle, three insulated type-K thermocouples described in section 7.1, were TIG-welded (Tungsten Inert Gas) onto the outside of the steel pipes of the engine. The first thermocouple was welded onto the vertical midpoint of the 20" steel pipe leading from the compressor to the combustor. The second thermocouple was TIG-welded onto the vertical midpoint of the 1.5" steel pipe between the combustor outlet and the turbine inlet. The third thermocouple was placed on the outside wall of the exhaust pipe leading from the turbine outlet, a horizontal distance of 7.62 cm (3") away from the outlet.

There are several advantages to placing the thermocouples on the outside walls of the pipes – namely that the air flow is not perturbed by a temperature measuring device immersed in the flow. Also, it is easier to install the thermocouples on the outside wall rather than devising a way to install the thermocouples inside of the pipes.

It is known that the thermocouples measure the temperature of the outside of the pipe walls and not the actual bulk mean air temperature. However, the bulk mean temperature can be calculated from the measured outside pipe wall temperature and the known flow characteristics. In the following sections a method for determining the bulk mean air temperature is developed, starting with the analysis of a thermal circuit.

6.1 The Thermal Circuit

In heat transfer problems, it is common to think of the thermal interactions to be acting through a thermal circuit. The temperature gradient in heat transfer problems represents the potential difference between two media and the resistive elements represent the thermal resistance of the heat transfer mode. A schematic diagram of the cross-sectional thermal circuit for this project is illustrated in Figure 14.

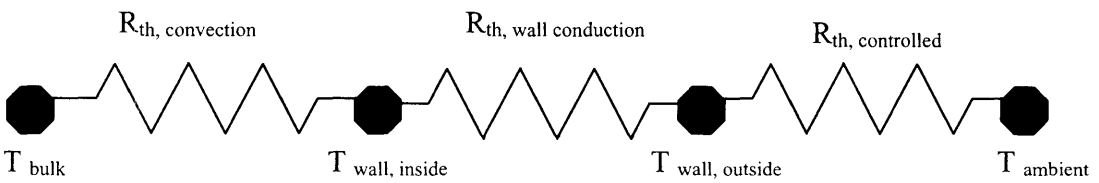

Figure 14: Schematic diagram of thermal circuit in gas turbine configuration.

The first resistive element from the left, $R_{th,\ convection}$ represents the thermal resistance due to convective heat transfer between the air at bulk mean temperature, T_{bulk}, and the inside wall of the pipe at temperature, $T_{wall,\ inside}$. The middle resistive element, $R_{th,\ wall\ conduction}$ represents the thermal resistance due to conductive heat transfer through the pipe wall driven by the temperature gradient within the wall. The temperature measured by the thermocouples is shown by, $T_{wall,\ outside}$. The third resistive element, $R_{th,\ controlled}$ represents the controlled thermal resistance between the outside wall and the environment. This thermal resistance is referred to as 'controlled' because the heat flow from the pipe to the environment can be allowed to do so by natural convection heat transfer or by conduction through a heat resistant material. In the next section, it is shown that heat transfer by conduction through high-temperature insulation is most useful for estimating the heat flow rate. $T_{ambient}$ is the measured ambient temperature.

By virtue of the first law of thermodynamics, thermal energy must be conserved through the pipe cross-section. That is to say, the heat flow rate through all thermally resistive elements is equal. Therefore, if a heat flow rate through a known thermal resistance is determined, it is possible to establish a radial temperature profile as a function of thermal resistance and heat flow rate. The desired temperatures at the nodes shown in Figure 14 can be solved for from the radial temperature profile. In the next section, a method is developed for estimating the heat flow rate.

6.2 Estimation of Heat Flow Rate

Since the temperature of the outside pipe wall is known from the thermocouple reading and the ambient temperature is also measured, it is useful to begin the analysis of the thermal circuit between this temperature gradient. Because the thermal resistance can either be convective or conductive, an analysis of each resistive case is required to determine the most accurate heat flow rate. The analysis begins with a study of natural convection from the pipe to the environment.

6.3 Natural Convection on Horizontal and Vertical Cylinders

Convective heat transfer can be calculated from Newton's Law of Cooling,

$$\dot{Q} = h_o A_o \left(T_{wo} - T_\infty\right), \tag{46}$$

where, $\dot{Q}$ is the heat transfer rate. The variable, h_o represents the convective heat transfer coefficient defined on the outside surface area of the pipe, A_o. The heat transfer rate varies with the temperature gradient, $\left(T_{wo} - T_\infty\right)$, between the pipe surface and that of the environment, i.e. at infinity, and the characteristics of the fluid flow field. Determining the value of the heat transfer coefficient requires the study of the dimensionless Nusselt number as it applies to this geometrical configuration.

The natural convection of thermal energy from the vertical wall of a cylinder is approximated to be the same as that of a vertical plate if the thermal boundary layer is

thin relative to the cylinder length [7]. This approximation is valid for the pipe leading from the compressor to the combustor and the pipe leading from the combustor to the turbine. The Nusselt number for a vertical plate is calculated from,

$$\overline{Nu_L} = 0.678 Ra_L^{1/4} \left(\frac{Pr}{0.952 + Pr} \right)^{1/4} . \tag{47}$$

The Nusselt number for natural convection on a horizontal cylinder, i.e. the turbine exhaust pipe, is calculated from,

$$\overline{Nu_D} = 0.36 + \frac{0.518 Ra_D^{1/4}}{\left[1 + (0.559/Pr)^{9/16}\right]^{16/9}}, \tag{48}$$

and is valid for

$$10^{-4} \leq Ra_D \leq 10^{9}.$$

$\overline{Nu}$ is the Nusselt number applicable for the entire length or diameter of the pipe, Ra_L is the Rayleigh number applicable for the entire length of the pipe, and Pr is the Prandtl number of the air. The Rayleigh number is represented by,

$$Ra_L = \frac{g\beta \Delta T L^3}{\nu \alpha}, \tag{49}$$

where, g is the acceleration due to gravity; ΔT is the temperature difference between the pipe wall and the air, β is the coefficient of thermal expansion equal to T_∞^{-1}, the inverse of air temperature at infinity; L is the pipe length; ν is the kinematic viscosity air; and α is the thermal diffusivity of air. The properties Pr, ν, and α of air are taken at the average temperature between the pipe wall and the air at infinity, shown by,

$$\overline{T} = \frac{T_w + T_\infty}{2} . \tag{50}$$

The Nusselt number for this configuration is also shown by,

$$\overline{Nu_L} = \frac{h_o L}{k_{air}}, \tag{51}$$

where, k_{air} is the thermal conductivity of air. The convective heat transfer coefficient for the vertical pipes is determined by combining equations (47) and (51) and solving for h_o. The Nusselt number for a horizontal pipe is also given by,

$$Nu_D = \frac{h_o D}{k_{air}}. \tag{52}$$

The convective heat transfer coefficient is determined in the same way as before, but it will not have the same numeric value as that for the vertical pipes.

The local thermal boundary layer thickness, $\delta(x)$, as it varies with the vertical distance of the plate, x, is determined for this configuration from

$$\frac{\delta(x)}{x} = Gr_x^{-1/4}\left[f(\mathrm{Pr})\right]^{1/4} \quad , \tag{53}$$

where, $f(\mathrm{Pr})$ is a function of Pr^{-1} and Pr^{-2} and the local Grashof number, Gr_x is shown by

$$Gr_x = \left(\frac{\beta g \Delta T_s}{\nu^2}\right). \tag{54}$$

But the local Nusselt number is

$$Nu_x = Gr_x^{-1/4}\left[f(\mathrm{Pr})\right]^{1/4} \tag{55}$$

and if the Nusselt number is solved for over the entire length, L, of the plate, the approximate boundary layer thickness becomes

$$\delta(L) = \overline{Nu_L} L. \tag{56}$$

It is important to note that the boundary layer is thickest at a length, L.

It must be noted that this analysis may not yield accurate results for two reasons. First, it is safe to assume that the thermal boundary layer thickness on the compressor-to-combustor pipe will be much less than the pipe length. However, this assumption may not be valid for the 3.81 cm (1.5") long pipe leading from the combustor to the turbine. Nevertheless, assuming both vertical pipes satisfy the thermal boundary layer thickness condition, the second reason as to why the natural convection analysis does not yield accurate results is more due to the calculation of the Nusselt number. The Nusselt number dependency on the Rayleigh number, which depends on the average temperature between the outside pipe wall and the air at infinity, is the limiting factor in this problem. It is expected that due to the anticipated air temperatures inside the engine on the order of 700 to 800 K, the engine will warm the testing environment so that the air temperature at infinity is no longer constant and thus, difficult to measure accurately. Therefore, to determine the heat flow rate from the outer pipe wall to the environment a conductive thermal resistance is imposed on the temperature differential between the pipe and the environment.

6.4 Conductive Thermal Resistance of Pipe Insulation

Another method of controlling the heat flow rate from the pipe to the environment is by introducing a known conductive thermal resistance between the two thermal nodes. Radial heat conduction in a tube can be calculated from the Fourier Conduction Law,

$$\dot{q} = -k\left(\frac{dT}{dr}\right) \tag{57}$$

where, $\dot{q}$ is the heat flux, k is the thermal conductivity of the conducting material, and $\left(\frac{dT}{dr}\right)$ is the temperature gradient through the thickness of the material. It must be noted that $\dot{q}$ is not constant due to the changing area through which heat flows. Taking into account the changing heat flux, for a pipe, the Fourier Conduction Law is given by,

$$\dot{Q} = \frac{T_{wo} - T_{\infty}}{R_{\text{th, conduction}}}, \tag{58}$$

where, T_{wo} is the temperature of the outer wall of the pipe measured by the thermocouple. The term in the denominator, $R_{\text{th, conduction}}$ is the conductive thermal resistance, shown by

$$R_{\text{th, conduction}} = \frac{\ln(r_o / r_i)}{2\pi k_I L}, \tag{59}$$

where, r_o is the outer radius of the pipe insulation, r_i is the inner radius of the pipe insulation or simply, the outer radius of the pipe itself, k_I is the thermal conductivity of the insulation, and L is still the length of the pipe. By combining equations (58) and (59) the convenience of implementing this conductive thermal resistance method should be apparent. In equations (58) and (59) the only unknown variable is $\dot{Q}$ because the other variables are specified material properties or measured quantities. The issue with the air temperature at infinity is resolved because it can be found by two different methods. The first method to determine T_{∞} is by assuming that the surrounding air temperature is not significantly affected by the insulated engine components. However, the most accurate result is obtained by measuring the temperature of the outside of the insulation, say with another thermocouple. Due to the relative ease of obtaining T_{∞} by either method, it is recommended that both are implemented and compared for accuracy.

For this project, the conductive thermal resistance is manifested in a high-temperature insulating material manufactured by the Thermo-Tec Automotive Products. The material is made from woven silica and its thermal conductivity, as specified by the supplier, is 0.3399 $\frac{\text{Btu} \cdot \text{in}}{\text{hr} \cdot \text{ft}^2 \cdot ^{\circ}\text{F}}$, which is approximately 0.0490 $\frac{\text{W}}{\text{m} \cdot \text{K}}$. Now that a method

has been developed to determine the heat flow rate through the controlled resistive element in the thermal circuit, the thermal resistance between the outer pipe wall and the inner pipe wall can be evaluated.

6.5 Conductive Thermal Resistance of Pipe Wall

The result of the combination of equations (58) and (59) is useful in the determination of the conductive thermal resistance in the pipe wall. The Fourier Conduction Law for this resistive element is,

$$\dot{Q} = \frac{T_{wi} - T_{wo}}{R_{\text{th, wall}}}, \tag{60}$$

where, T_{wi} is the temperature of the inner wall of the pipe. The conductive thermal resistance of the wall, $R_{\text{th, wall}}$ is shown by,

$$R_{\text{th, wall}} = \frac{\ln(R_o / R_i)}{2\pi k_S L}, \tag{61}$$

where, R_o is the pipe outer radius, R_i is the pipe inner radius, and k_S is the temperature dependent thermal conductivity of steel. The thermal conductivity will reflect the temperature of the steel at each thermocouple location due to the varying air temperatures in the engine.

From equation (60), T_{wi} is shown by,

$$T_{wi} = \dot{Q} R_{\text{th, wall}} + T_{wo}, \tag{62}$$

where, $\dot{Q}$ is shown by the result of the combination of equations (58) and (59). Therefore, the inner wall temperature of the pipe is determined from the combination of equations (58) through (62) and shown by,

$$T_{wi} = \frac{k_I \ln(R_o / R_i)}{k_S \ln(r_o / r_i)}(T_{wo} - T_\infty) + T_{wo}. \tag{63}$$

Now that the model for determining the inner wall temperature of the pipe has been established, the convective thermal resistance between the bulk mean air temperature and the inner wall temperature is evaluated to find the bulk mean air temperature. The convective thermal resistance depends on the nature of the flow as well as the hydrodynamic development of the flow

6.6 Hydrodynamic and Thermal Entry Lengths

Since the working temperatures of the engine vary from 380 K to 800 K, the Prandtl number air varies from approximately 0.704 to 0.723. For fluids whose Prandtl number is less than unity, the effects of the Prandtl number on the thermal entry length are greater than for those fluids whose Prandtl number is much greater than unity. Due to the turbulent nature of the air flow in every component of the engine, it is expected that the thermal entry length of the air flow will be significantly less than 30 inner pipe diameters [8].

The hydrodynamic entry length, L_{entry}, for circular conduits in turbulent flow is given by

$$\left(\frac{L_{entry}}{D_i}\right)_{hy} = 1.359 Re^{1/4}. \tag{64}$$

The Reynolds number, Re_D, is given by

$$Re_D = \frac{4\dot{m}}{\pi D_i \mu}, \tag{65}$$

where $\dot{m}$ is the air mass flow rate, D_i is the inner diameter of the pipe, and μ is the temperature dependent viscosity of the air.

The resulting hydrodynamic entry length is useful in determining the Nusselt number correlation that will be implemented in the problem. It will be shown that the hydrodynamic entry lengths for each pipe are greater than the length of the pipe itself. As a result, the Nusselt number correlations reflect the fluid entry length behavior.

6.7 Determination of Bulk Mean Temperature from Convective Thermal Resistance

For this resistive element in the thermal circuit, Newton's Law of Cooling appears as,

$$\dot{Q} = h_i A_i (T_b - T_{wi}), \tag{66}$$

where A_i is the area of the inside wall of the pipe, h_i is the coefficient of convective heat transfer on the inside pipe wall, and T_b is the bulk mean air temperature. There are two unknown variables in equation (66), h_i and T_b. Therefore, to establish a model that solves for T_b, h_i must be determined first.

The coefficient of convective heat transfer defined on the inside surface of a circular conduit is determined from the nature of the fluid flow. As it will be shown in sections 6.10, 6.11, and 6.12, the air flow throughout the entire engine will be turbulent.

6.8 Nusselt Number Approximation for Determining Heat Transfer Coefficient

6.8.1 Nusselt Number for Fully Developed Flow

The Nusselt number for hydrodynamically fully developed turbulent flow in smooth circular conduits is calculated from the Gnielinski correlation that shows,

$$Nu_D = \frac{\frac{f}{8}(Re_D - 1000)Pr}{1 + 11.5\sqrt{\frac{f}{8}}(Pr - 1)}. \tag{67}$$

Equation (17) is valid for Reynolds numbers $2300 \le Re_D \le 5 \times 10^6$ and for Prandtl numbers, $0.5 \le Pr \le 2000$. The friction factor, f, is given by the correlation,

$$f = (0.790 \ln Re_D - 1.64)^{-2}. \tag{68}$$

6.8.2 Nusselt Number in Thermal Entry Length

Nusselt number solutions for the thermal entry length of a circular tube have been determined experimentally for *constant surface temperature* by Sleicher and Tribus [9] and for *constant heat rate* by Sparrow, Hallman, and Seigel [9]. The results from each situation are of equal importance to this analysis due to the relatively invariant results from the two experiments. Nusselt numbers in the thermal entry length of a circular tube for a constant heat rate can be extrapolated from Figure 15.

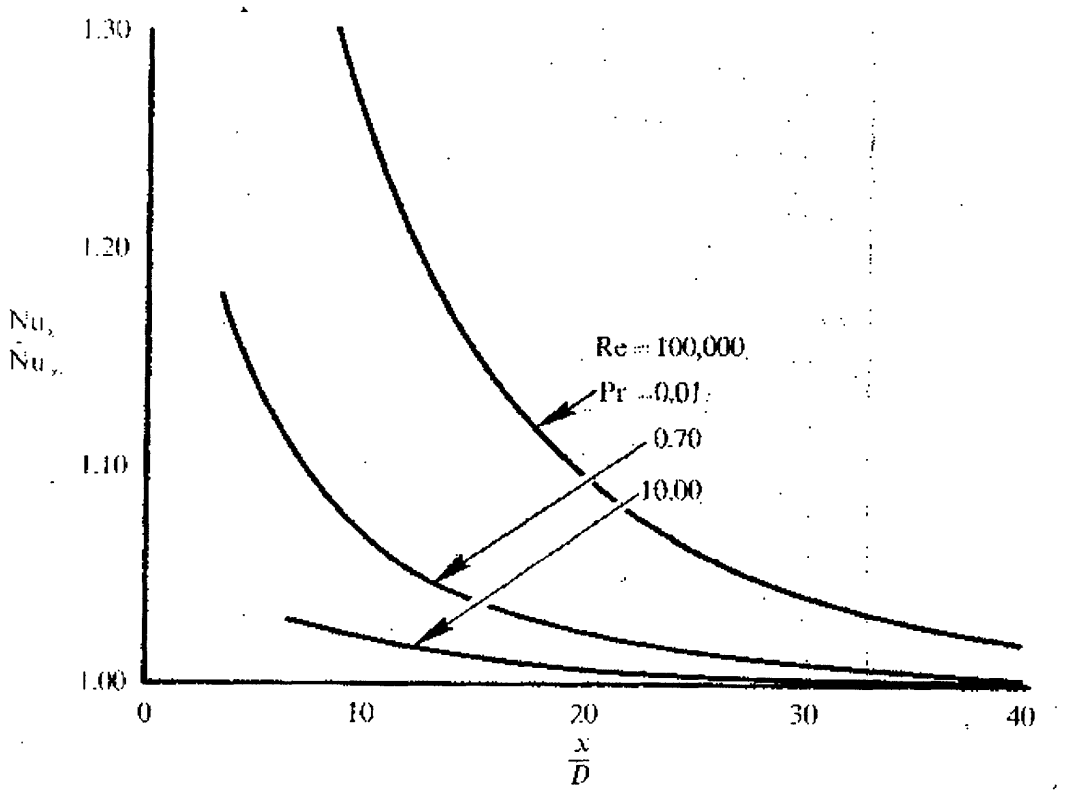

Figure 15: Nusselt numbers in thermal entry length of a circular tube, constant heat rate [9].

Plotted on the ordinate is the ratio of the mean local Nusselt number, Nu_x, to Nu_D determined from equation (17). On the abscissa lie the values of the ratio between axial position, x, and inner pipe diameter, D. The Reynolds number curve representing the Prandtl number, $Pr = 0.7$ is of the utmost interest. The Nusselt number curves for air, $Pr = 0.7$, show insignificant dependency on varying Reynolds number, as shown in Figure 16.

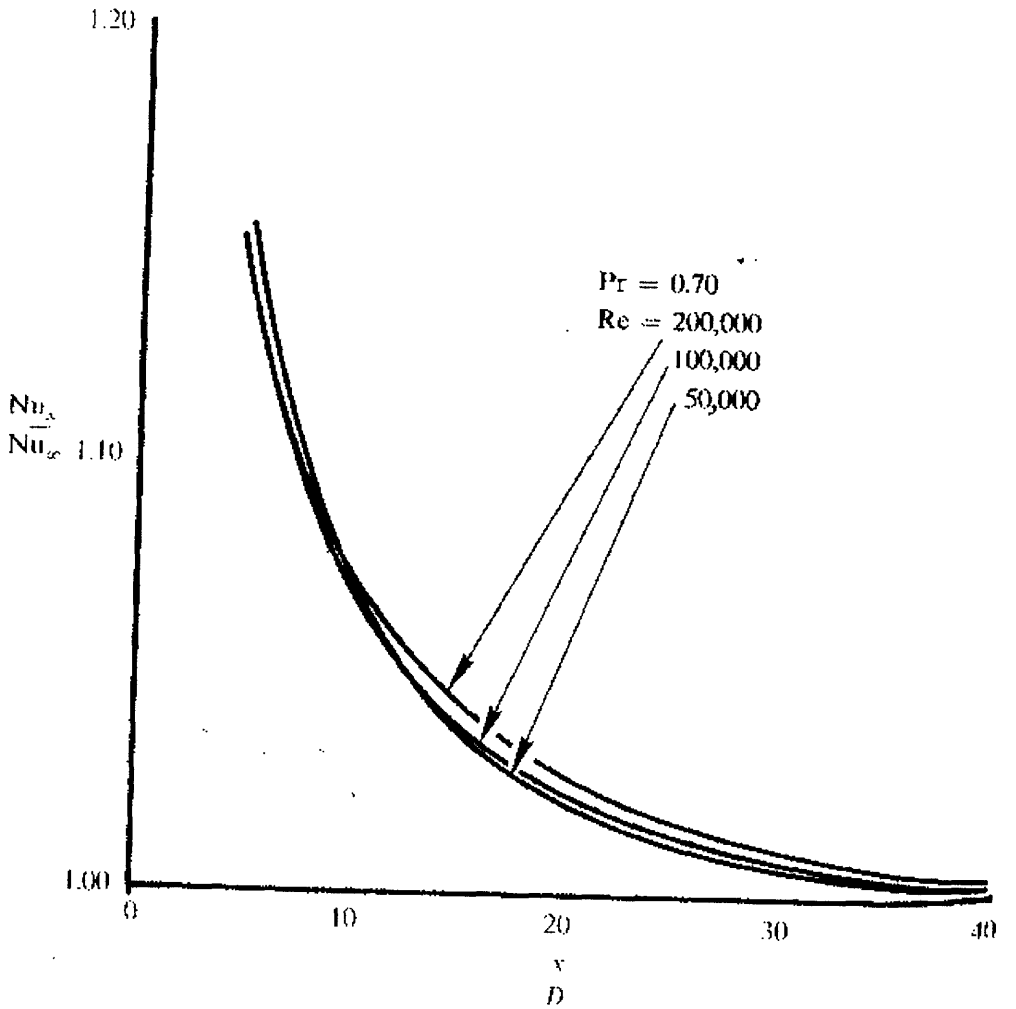

Figure 16: Nusselt numbers for air in the thermal entry length of a circular tube, constant heat rate [9].

The ratio of the two Nusselt numbers is determined from Figures 16 and 17 when the Reynolds number, equation (65), and the ratio of x and D are known. The Nusselt number for fully developed flow is determined from equation (67). Therefore, the only unknown parameter in this problem is the local Nusselt number, Nu_x. The local Nusselt number is given by the correlation,

$$Nu_x = \frac{h_i D_i}{k_{air}}. \tag{69}$$

The convective heat transfer coefficient is solved for from equation (69).

6.9 Applying the Heat Transfer Coefficient to Determine Bulk Mean Temperature

Solving Newton's Law of Cooling for the mean bulk temperature so that,

$$T_b = \frac{\dot{Q}}{h_i A_i} + T_{wi}, \tag{70}$$

and substituting the result of equation (63) for T_{wi} and the result of equation (58) for $\dot{Q}$, the bulk mean temperature is given by,

$$T_b = k_I \left[\frac{1}{h_i r_i \ln\left(\frac{r_o}{r_i}\right)} + \frac{\ln\left(\frac{R_o}{R_i}\right)}{k_s \ln\left(\frac{r_o}{r_i}\right)} \right] \left(T_{wo} - T_\infty\right) + T_{wo}. \tag{71}$$

Now that a general bulk mean temperature model has been established, it can be applied to the specific engine pipes.

6.10 Bulk Mean Air Temperature in Compressor-to-Combustor Pipe

The pipe leading from the outlet of the compressor to the inlet of the combustor has an inner diameter of 0.0407 m (1.603") and an outer wall diameter of 0.0483 m (1.903"). The thickness of the insulation is 0.001016 m (0.040"). However, the insulation is wrapped twice around the pipes so that the insulation thickness is actually, 0.002032 m (0.080"). The outer pipe radius, r_o with insulation is then 0.05033 m. The conductive thermal resistance is given by,

$$R_{\text{th, conduction}} = \frac{\ln(r_o / r_i)}{2\pi k_I L} = 0.263 \frac{\text{K}}{\text{W}} \quad . \tag{72}$$

Next, the thermal resistance of the pipe wall is evaluated. Recalling that the mean bulk air temperature is expected to be on the order of 388 K for this pipe, the thermal conductivity of steel at is approximately 60 $\frac{\text{W}}{\text{m} \cdot \text{K}}$. The resistance to conduction heat transfer in the pipe wall is given by,

$$R_{\text{th, wall}} = \frac{\ln(R_o / R_I)}{2\pi k_S L} = 8.94 \times 10^{-4} \frac{\text{K}}{\text{W}}. \tag{73}$$

To evaluate the convective heat transfer resistance in this pipe, first the Reynolds number is calculated to verify the nature of the fluid flow. The Reynolds number is given by

$$Re_D = \frac{4\dot{m}}{\pi D_i \mu} = 1.668 \times 10^5, \tag{74}$$

where, μ of air at 388 K is approximately $2.320 \times 10^{-5} \frac{\text{kg}}{\text{m} \cdot \text{s}}$. Next, the hydrodynamic entry length is calculated to determine the state of the fluid flow development. The hydrodynamic entry length is given by,

$$L_{\text{entry}_{\text{hy}}} = 1.359 D_i Re^{1/4} = 1.12 \text{ m} \tag{75}$$

Since the entry length is significantly greater than the length of the pipe, the flow is not fully developed. This result is reflected in the proceeding analysis.

The resulting Reynolds number from equation (74) indicates that the flow inside this pipe is turbulent. The friction factor for fully developed flow is given by,

$$f = (0.790 \ln Re_D - 1.64)^{-2} = 0.016155 \tag{76}$$

Therefore, the Nusselt number for fully developed flow is given by,

$$Nu_D = \frac{\frac{f}{8}(Re_D - 1000)Pr}{1 + 11.5\sqrt{\frac{f}{8}}(Pr - 1)} = 269.377 \tag{77}$$

The thermocouple is placed 0.254 m from the pipe inlet and the inner diameter of the pipe is 0.0407 m. Therefore,

$$\frac{x}{D} = 6.24, \tag{78}$$

and the ratio of the local to fully developed Nusselt numbers is found from Figure 15 to be approximately 1.4. The local Nusselt number is approximately,

$$Nu_x \approx 377.128. \tag{79}$$

The local convective heat transfer coefficient is given by

$$h_i = \frac{Nu_x k_{\text{air}}}{D} = 277.98 \frac{\text{W}}{\text{m}^2\text{K}}. \tag{80}$$

The convective heat transfer resistance is then given by

$$R_{\text{th, convection}} = \frac{1}{h_i A_i} = 0.055 \frac{\text{K}}{\text{W}}. \tag{81}$$

Finally, equation (71) is given by ,

$$T_b = 0.092(T_{wo} - T_\infty) + T_{wo}. \tag{82}$$

6.11 Bulk Mean Air Temperature in Combustor-to-Turbine Pipe

The pipe leading from the outlet of the combustor to the inlet of the turbine has an inner diameter of 0.0506 m (1.603") and an outer wall diameter of 0.0602 m (2.372"). The insulation thickness is still 0.002032 m (0.080"). The pipe length is 0.0381 m (1.5"). The predicted air temperature is approximately 800 K. The conductive thermal resistance for the insulation is given by,

$$R_{\text{th,conduction}} = \frac{\ln(r_o / r_i)}{2\pi k_I L} = 0.212 \frac{\text{K}}{\text{W}}. \tag{83}$$

The conductive thermal resistance of the pipe wall is given by,

$$R_{\text{th, wall}} = \frac{\ln(R_o / R_i)}{2\pi k_S L} = 0.0181 \frac{\text{K}}{\text{W}}, \tag{84}$$

where, k_S at 800 K is approximately 40 $\frac{\text{W}}{\text{m} \cdot \text{K}}$.

To determine the nature of the fluid flow, the Reynolds number is given by,

$$Re_D = \frac{4\dot{m}}{\pi D_i \mu} \Rightarrow 8.394 \times 10^4. \tag{85}$$

where the viscosity of air at 800 K is $3.747 \times 10^{-5} \frac{\text{kg}}{\text{m} \cdot \text{s}}$. As expected, the air flow remains turbulent. For this pipe the hydrodynamic entry length is given by,

$$L_{\text{entry}_{\text{hy}}} = 1.359 D_i Re^{1/4} = 1.17 \text{ m} \tag{86}$$

As before, the entry length is significantly greater than the length of the pipe, so the flow is not fully developed.

The friction factor for fully developed flow is given by,

$$f = (0.790 \ln Re_D - 1.64)^{-2} = 0.01869 \tag{87}$$

Therefore, the Nusselt number for fully developed flow is given by,

$$Nu_D = \frac{\frac{f}{8}(Re_D - 1000)Pr}{1 + 11.5\sqrt{\frac{f}{8}}(Pr - 1)} = 286.251 \tag{88}$$

The thermocouple is placed 0.019 m from the combustor outlet and the inner diameter of the pipe is 0.0506 m so that,

$$\frac{x}{D} = 0.375. \tag{89}$$

It is not possible to determine a definite Nusselt number ratio from Figure 15, because the pipe diameter is much greater than its length. However, it is known that Nusselt numbers are indefinitely high at the beginning of flow, i.e. for axial positions close to zero, and decrease with length as reflected by Figure 15 [9]. As a result, it is assumed that the convective heat transfer coefficient is essentially infinite in this section of the pipe so that

$$R_{\text{th, convection}} = \frac{1}{h_i A_i} \to 0 \frac{\text{K}}{\text{W}}. \tag{90}$$

Since the resistance to heat transfer by convection is negligible equation (71) becomes

$$T_b = \frac{k_I}{k_s}\left[\frac{\ln\left(\frac{R_o}{R_i}\right)}{\ln\left(\frac{r_o}{r_i}\right)}\right](T_{wo} - T_\infty) + T_{wo}. \tag{91}$$

Substituting the known variable values into (91) the bulk mean temperature is given by,

$$T_b = 0.0427(T_{wo} - T_\infty) + T_{wo}. \tag{92}$$

6.12 Bulk Mean Air Temperature in Exhaust Pipe

The exhaust pipe has an inner diameter of 0.0603 m (2.375") and outer diameter of approximately 0.0635 m (2.5"). The insulation thickness remains 0.002032 m (0.080"). The pipe length is approximately 0.254 m (10") horizontally and 0.914 m (36")

vertically. The predicted exhaust air temperature is 700 K. The conductive thermal resistance for the insulation is given by,

$$R_{\text{th, conduction}} = \frac{\ln(r_o / r_i)}{2\pi k_I L} = 0.403 \frac{\text{K}}{\text{W}}. \tag{93}$$

The conductive thermal resistance of the pipe wall is given by,

$$R_{\text{th, wall}} = \frac{\ln(R_o / R_i)}{2\pi k_S L} = 7.2 \times 10^{-4} \frac{\text{K}}{\text{W}}, \tag{94}$$

where, k_S at 700 K is approximately 45 $\frac{\text{W}}{\text{m} \cdot \text{K}}$.

To determine the nature of the fluid flow, the Reynolds number is given by,

$$Re_D = \frac{4\dot{m}}{\pi D_i \mu} \Rightarrow 8.1 \times 10^4. \tag{95}$$

where the viscosity of air at 700 K is $3.257 \times 10^{-5} \frac{\text{kg}}{\text{m} \cdot \text{s}}$. The air flow remains turbulent. For this pipe the hydrodynamic entry length is given by,

$$L_{\text{entry}_{\text{hy}}} = 1.359 D_i Re^{1/4} = 1.38 \text{ m} \tag{96}$$

Again, the entry length is significantly greater than the length of the pipe, so the flow is not fully developed.

The friction factor for fully developed flow is given by,

$$f = (0.790 \ln Re_D - 1.64)^{-2} = 0.01882 \tag{97}$$

Therefore, the Nusselt number for fully developed flow is given by,

$$Nu_D = \frac{\frac{f}{8}(Re_D - 1000)Pr}{1 + 11.5\sqrt{\frac{f}{8}}(Pr - 1)} = 159.99 \tag{98}$$

The thermocouple is placed 0.076 m (3") from the turbine outlet and the inner diameter of the pipe is 0.060 m so that,

$$\frac{x}{D} = 1.26 . \tag{99}$$

Again, it is not possible to determine a definite Nusselt number ratio from Figure 15, because the pipe diameter is on the same order as the distance to the thermocouple. For the same reasons as with the combustor-to-turbine pipe, it is assumed that the convective heat transfer coefficient is infinite in this section of the pipe so that equation (91) can be applied again. Substituting the known variable values into (91) the bulk mean temperature is given by,

$$T_b = 0.00136(T_{wo} - T_\infty) + T_{wo} . \tag{100}$$

7. Temperature Measurement System

7.1 Thermocouple Selection

The temperature sensors selected for this project are Type K thermocouples. Omega Engineering, Inc. manufactures the sensors. This common thermocouple type consists of a Nickel-Chromium alloy, referred to as Chromel, and a Nickel-Aluminum alloy, referred to as Chromel. Figure 17 is a schematic diagram of the thermocouple used in this project.

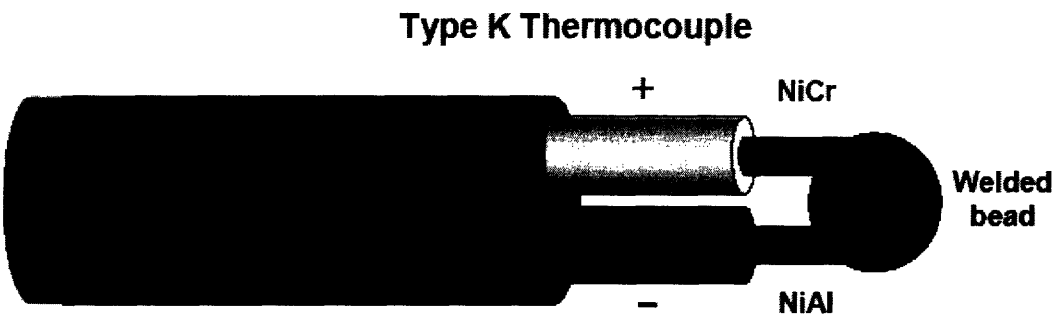

Figure 17: Insulated Type K thermocouple wire [10].

The welded bead in this experiment was achieved by TIG welding the two alloys together and then welding the unit onto the engine pipes in the same manner. The insulation surrounding the alloy wires is made from High Temperature Glass that is rated to a temperature of 704 C, well within the temperature limits of this experiment. The American Wire Gauge (AWG) Number is 20 for the thermocouples, which is equivalent to a wire diameter of 8.175×10^{-4} m (0.0323").

The Type K thermocouple was selected based on its variation of junction voltage with temperature relative to other thermocouple types and its usability for wide temperature range. Figure 18 depicts the thermocouple junction voltage sensitivity to changes in temperature.

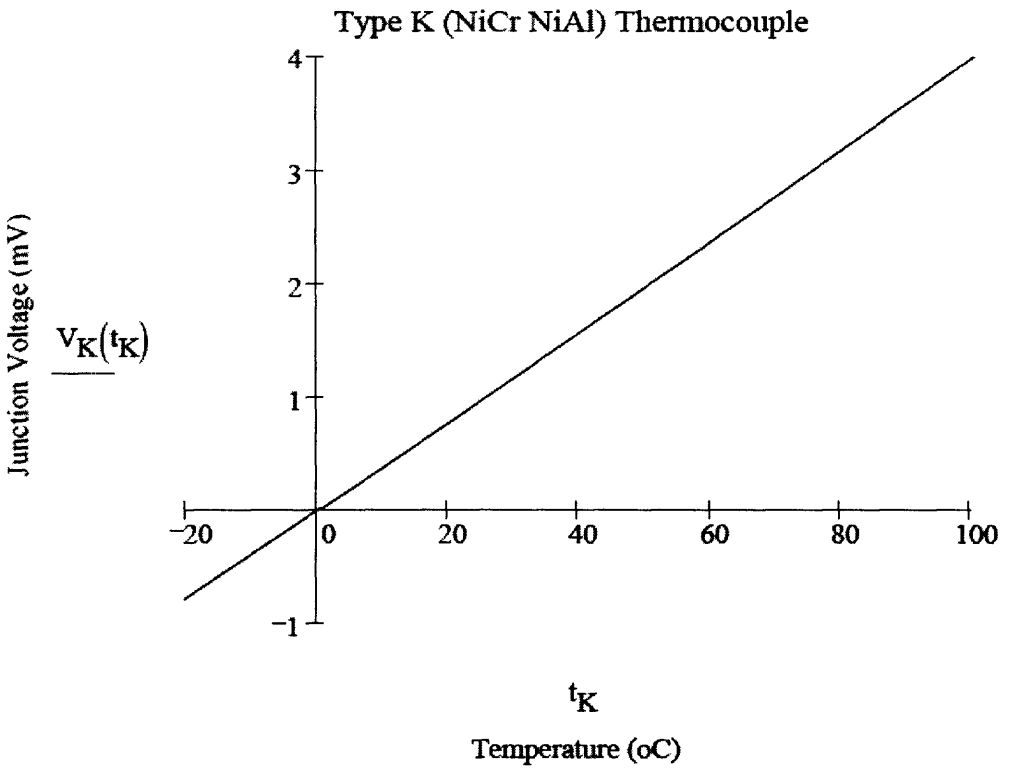

Figure 18: Plot of Type K thermocouple junction voltage response to temperature [10].

The junction voltage response to temperature is conveniently linear. Another advantage of using the Type K thermocouple is due its effectiveness for a wide temperature range. The junction voltage response to temperature for the range of -270 to 1372 C, as shown in Figure 19, remains linear.

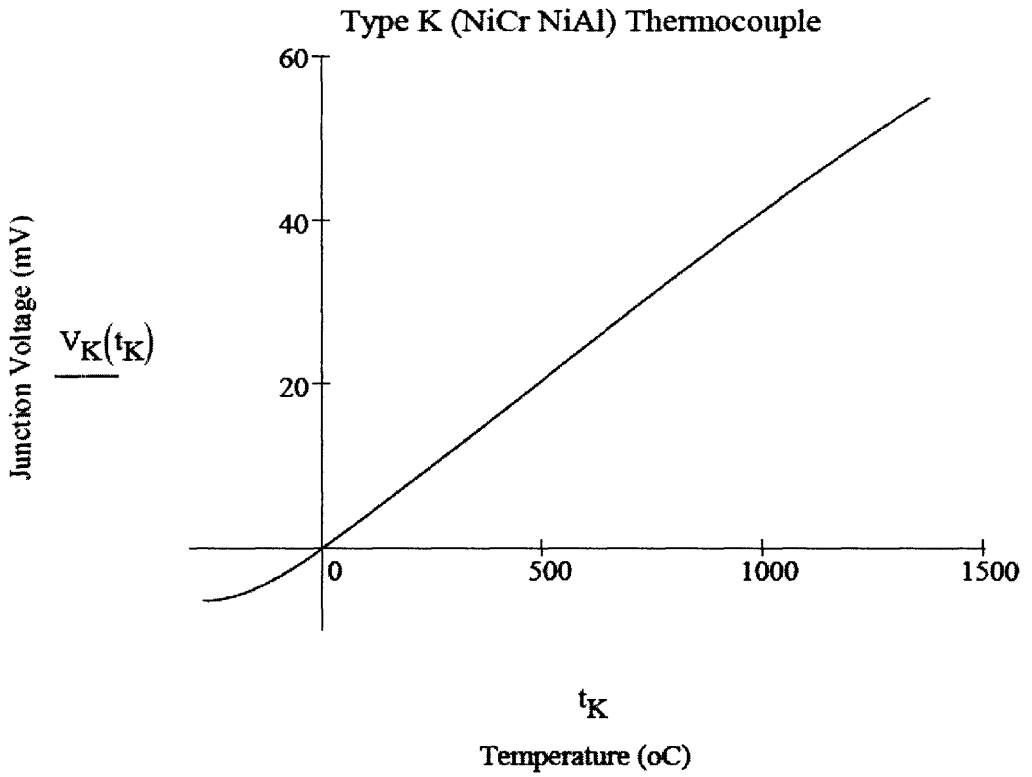

Figure 19: Plot of Type K thermocouple junction voltage response to wide temperature range [10].

Finally, the Type K thermocouples were compared to other thermocouple types. Figure 20 illustrates the comparison of five common thermocouples: Type J, Type K, Type B, and Type E. The junction voltage response to temperature and temperature range of the Type K thermocouple relative to that of the other types was the most critical parameters by which the Type K sensors were selected. Clearly, the Type K thermocouples account for the greatest temperature range and junction sensitivity.

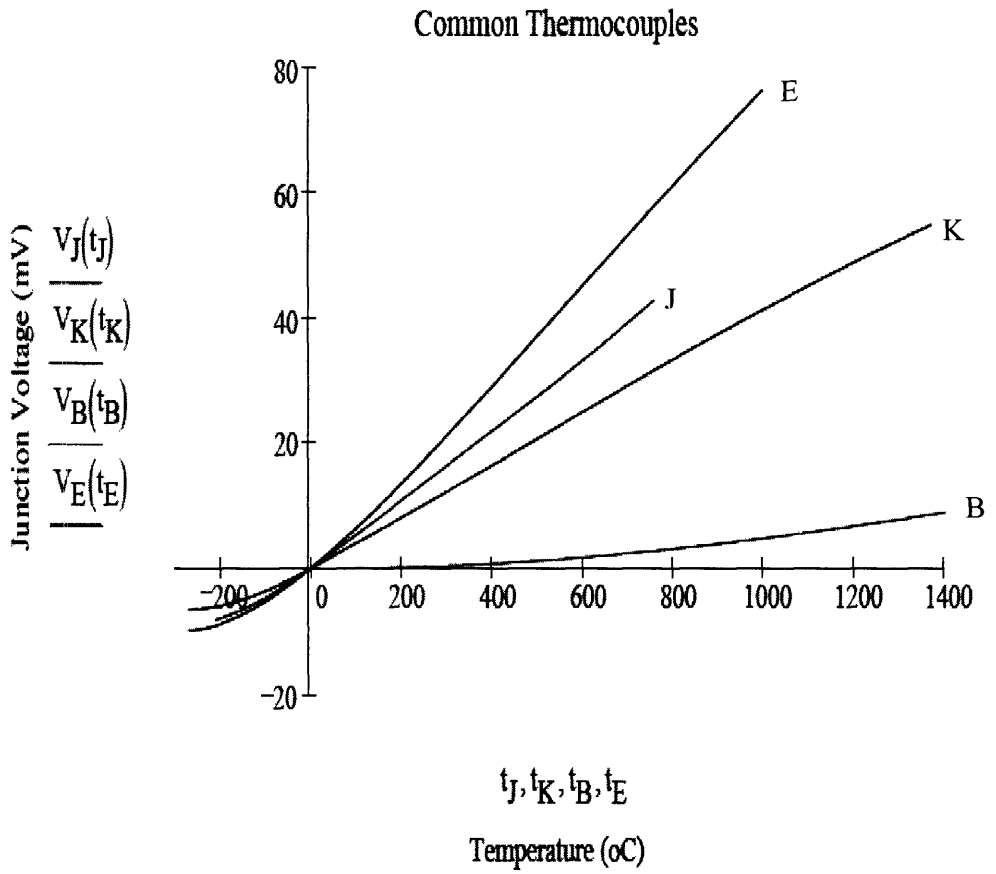

Figure 20: Comparison of various thermocouple types' junction voltage response to temperature [10].

7.2 Temperature Indicators

The thermocouple wires are connected to three temperature indicators manufactured by Omega Engineering, Inc. Two indicators are model DP460-T and have a range of -999 to 9,999 C with a 0.1 C auto-resolution and an accuracy of 0.5 C. No calibration is required to switch between thermocouple types. The third indicator is a model DP462-T meter that has the added ability to switch between up to six sensor inputs of the same type with its multi-input option.

8. Conclusion and Recommendations

The gas-turbine engine has been completely assembled and is ready for testing. The fuel system has been completed and integrated into the engine. The cooling and lubrication system has also been completed, using a cordless power drill as a power source for the oil pump. The model for determining the mean bulk air temperature has been developed for each of the stages of the cycle. The temperature model can be used for determining both the transient and steady-state bulk mean temperature. However, the current instrumentation can only be used for accurate steady-state results. Therefore, if accurate transient state data are desired, it is recommended that instrumentation with the ability to record data at high frequencies be integrated into the project.

In addition to measuring the air temperature at different stages of the cycle, it may also be useful to measure the air pressure at different stages of the cycle. It is recommended that the compressor outlet pressure be measured to determine the *actual* outlet pressure. Furthermore, it is recommended that the inlet and outlet pressure of the combustion chamber be measured to determine the pressure loss in the chamber. This result will be useful in the combustion chamber efficiency analysis. It must be noted that the pressure measuring instruments be rated to the working temperatures of the gas-turbine engine. It is also possible to design a capillary tubing system that reduces the temperature of the air that the pressure gauges are measuring.

Currently, the temperature of air at infinity is assumed to be the ambient temperature because the engine components have all been insulated. However, if a thermocouple or other temperature measuring device is placed on the outside of the insulation, the most accurate heat flow rate through the insulation can be determined. The heat flow rate from the insulation temperature can be compared to the result of heat flow rate from the ambient temperature.

9. References

[1] Keane Nishimoto, *Design of an Automobile Turbocharger Gas Turbine Engine*, Cambridge, MA: Massachusetts Institute of Technology, 2003.

[2] Lauren Tsai, *Design and Performance of a Gas-Turbine Engine from an Automobile Turbocharger*, Cambridge, MA: Massachusetts Institute of Technology, 2004.

[3] Ernest G. Cravalho & Joseph L. Smith, Jr., *Engineering Thermodynamics*, Cambridge, MA: Massachusetts Institute of Technology, 1981.

[4] Meherwan P. Boyce, *Gas Turbine Engineering Handbook,* Houston, TX: Gulf Publishing Company, 1982.

[5] Ian Benett. *Gas Turbines*. http://www.gasturbine.pwp.blueyonder.co.uk

[6] Engineers Edge. http://www.engineersedge.com/pumps/positve_disp_pump_char.htm

[7] John H. Lienhard, IV & John H. Lienhard, V, *A Heat Transfer Textbook Third Edition*, Cambridge, MA: Phlogiston Press, 2004.

[8] Ernest G. Cravalho, Joseph L. Smith, Jr., John G. Brisson II, Gareth H. McKinley, *An Integrated Approach to Thermodynamics, Fluid Mechanics, and Heat Transfer*, Cambridge, MA: Oxford University Press, 2005.

[9] W.M. Kays, *Convective Heat and Mass Transfer*, New York: McGraw-Hill Book Company, 1980.

[10] Ian Hunter, *2.671 Measurement and Instrumentation Lecture Notes,* Cambridge, MA: Massachusetts Institute of Technology, 2005.

[11] Jeff Tyson. *How Grills Work.* http://home.hostuffworks.com/grill3.htm

[12] Karim Nice. *How Turbochargers Work.* http://auto.howstuffworks.com/turbo.htm

Appendix

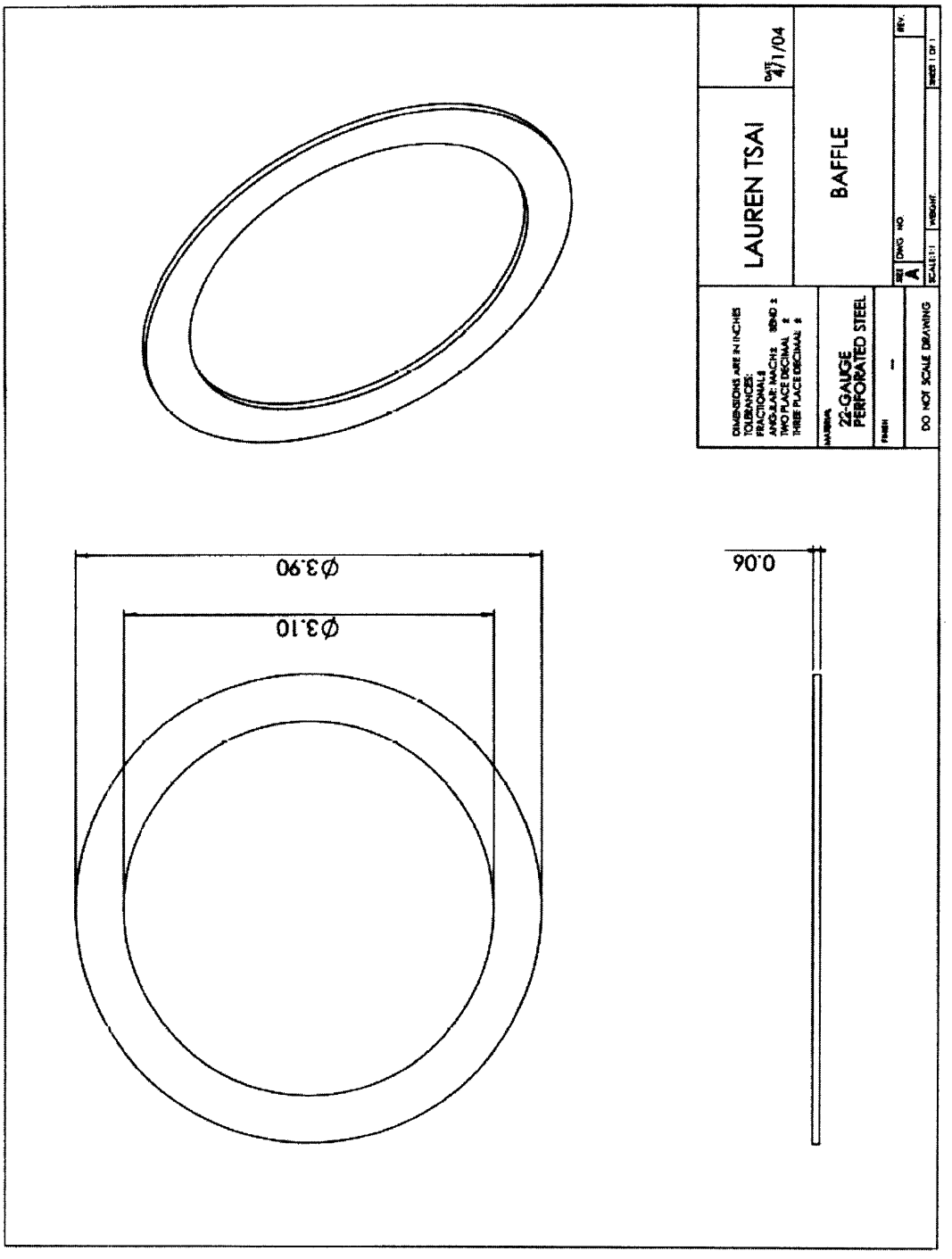

Figure 21: Baffle Part Drawing [2].

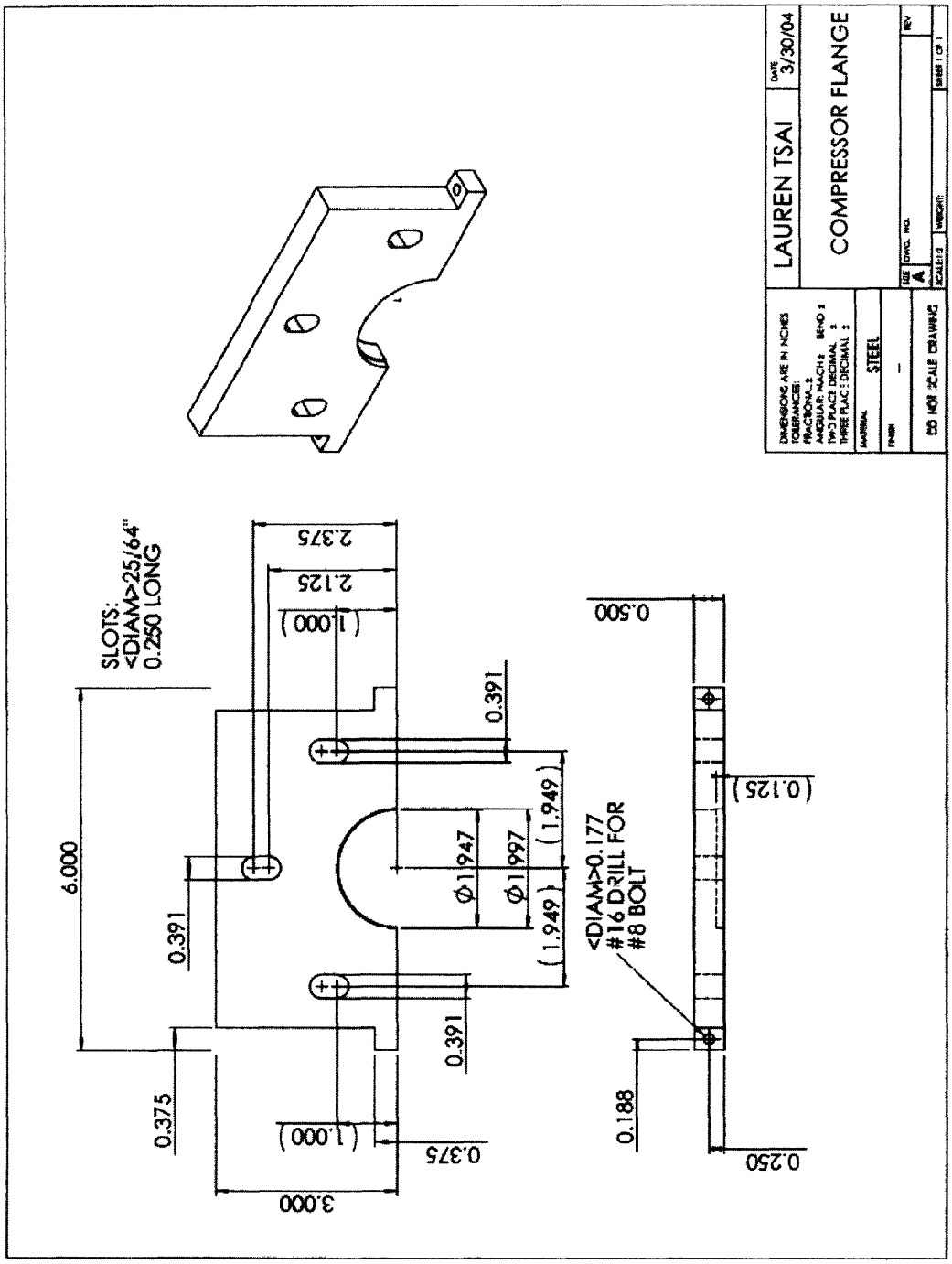

Figure 22: Compressor Flange Part Drawing [2]

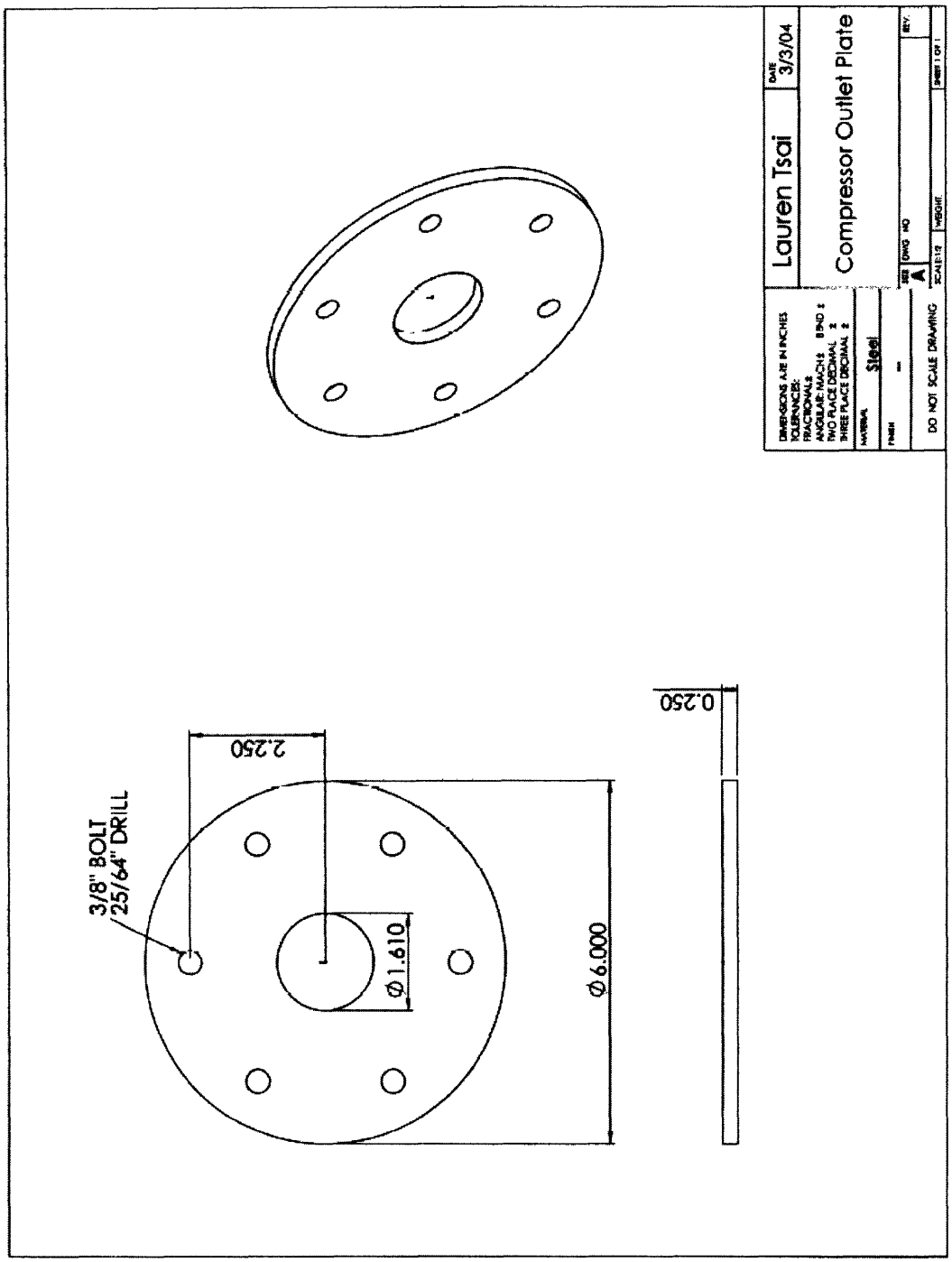

Figure 23: Compressor Outlet Plate Drawing [2]

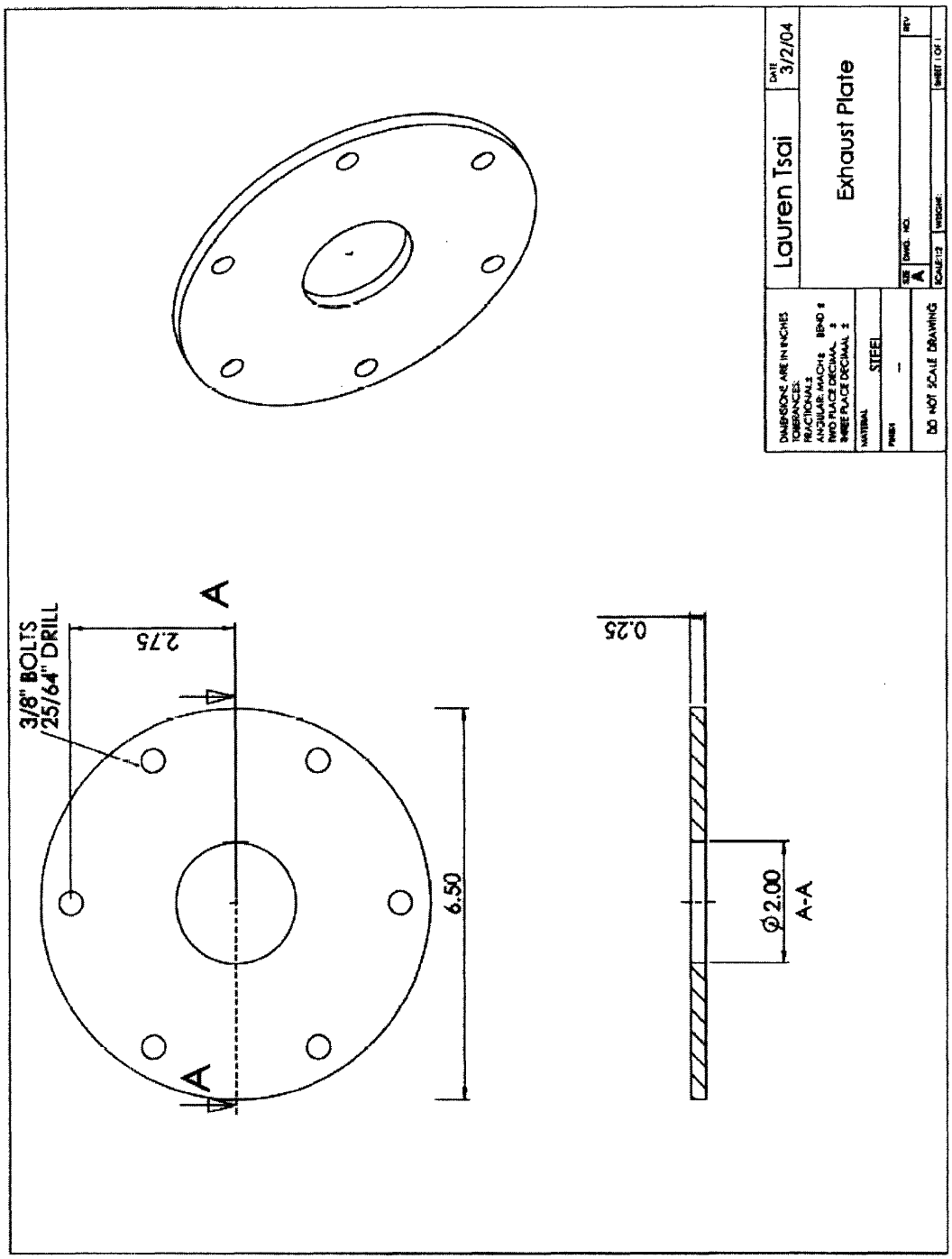

Figure 24: Exhaust Plate Part Drawing [2]

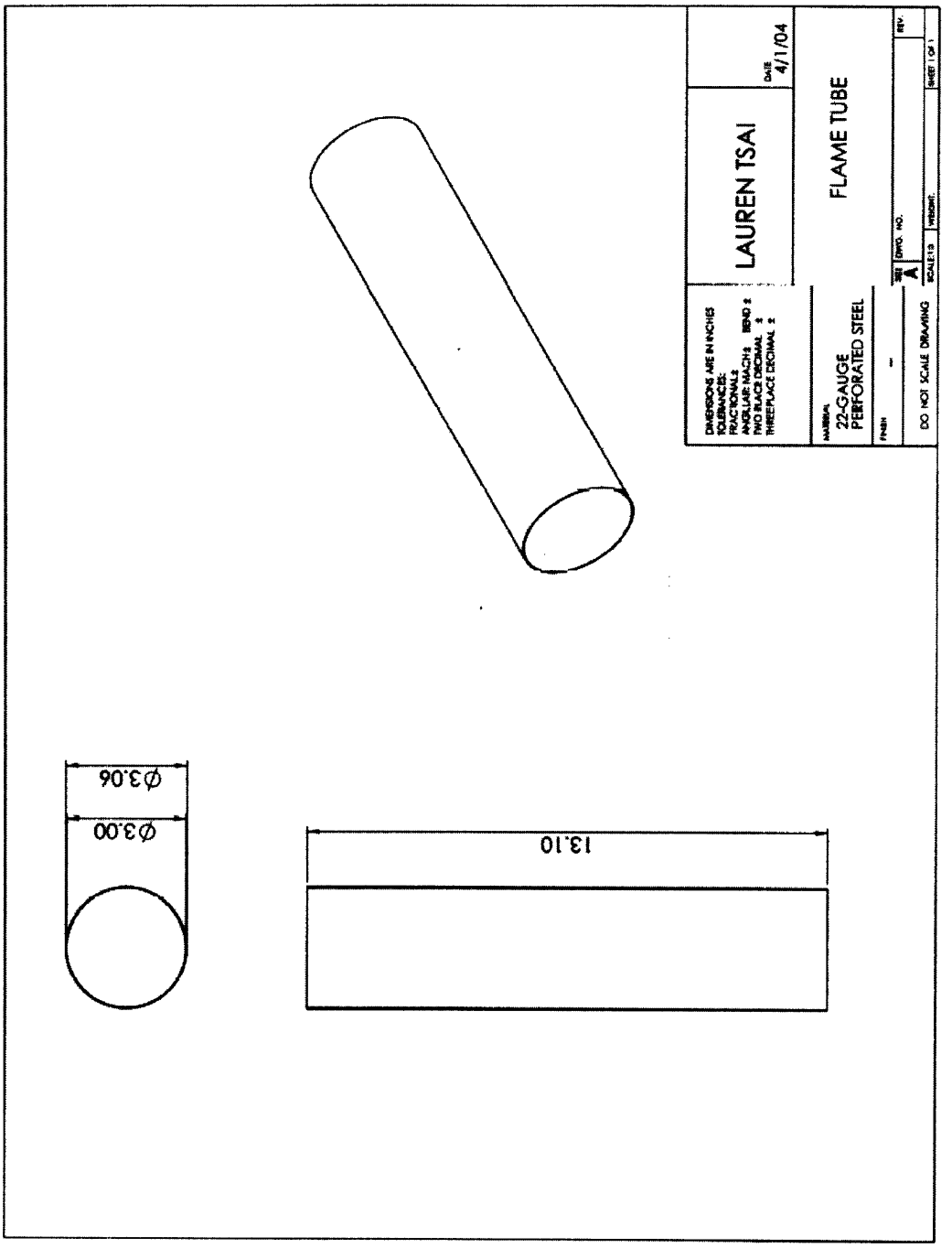

Figure 25: Flame Tube Part Drawing [2]

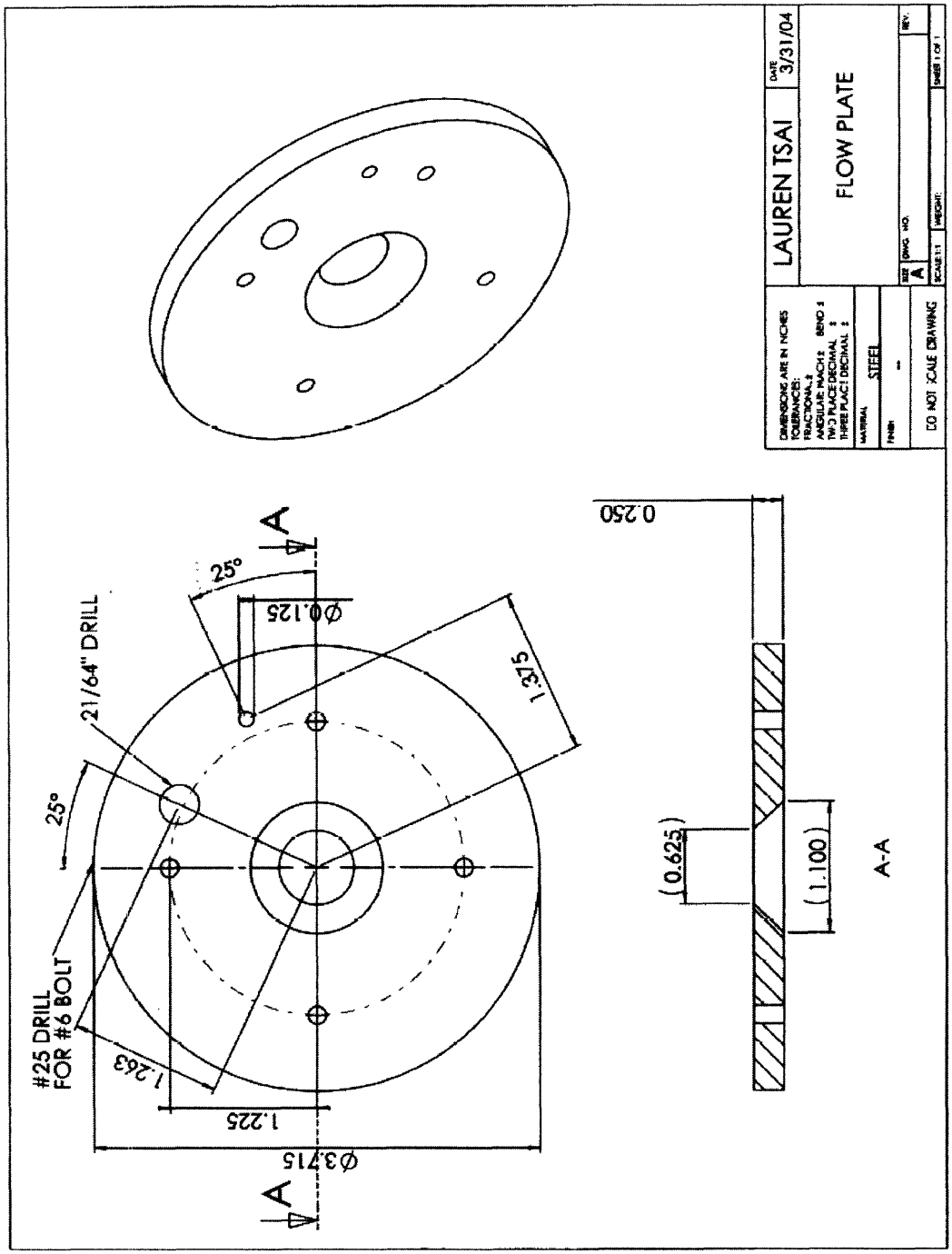

Figure 26: Flow Plate Part Drawing [2]

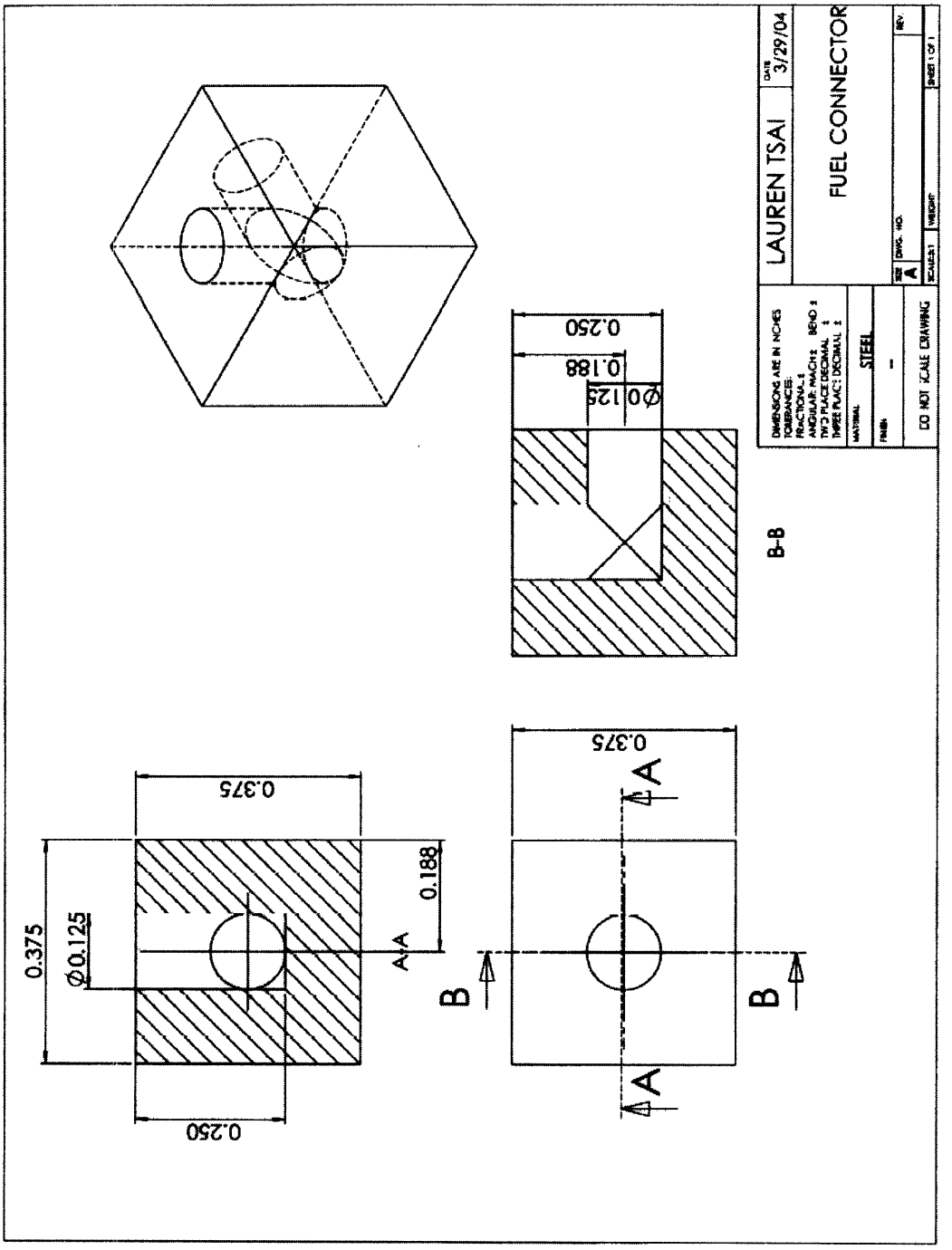

Figure 27: Fuel Hook Connector Block [2]

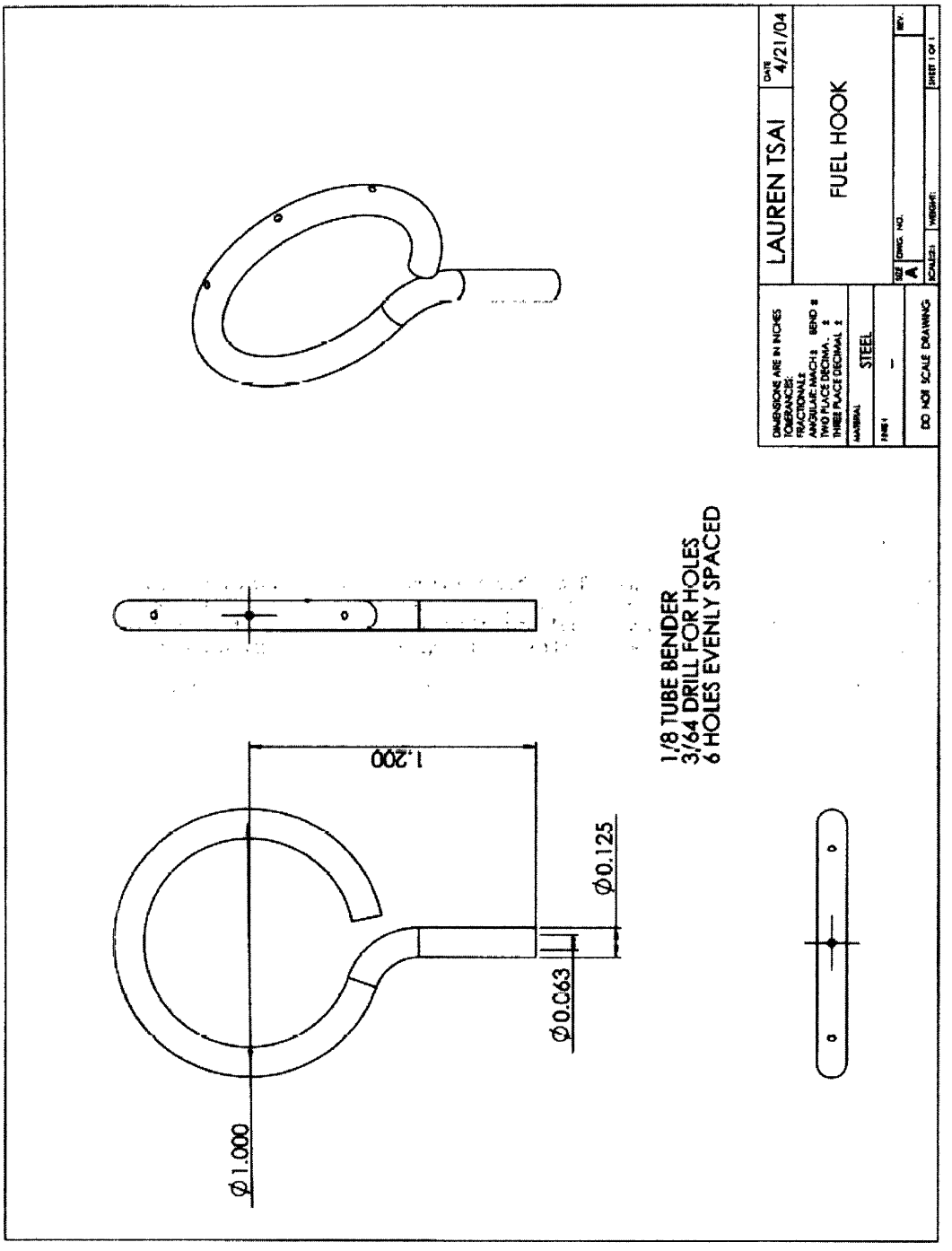

Figure 28: Fuel Hook Part Drawing [2]

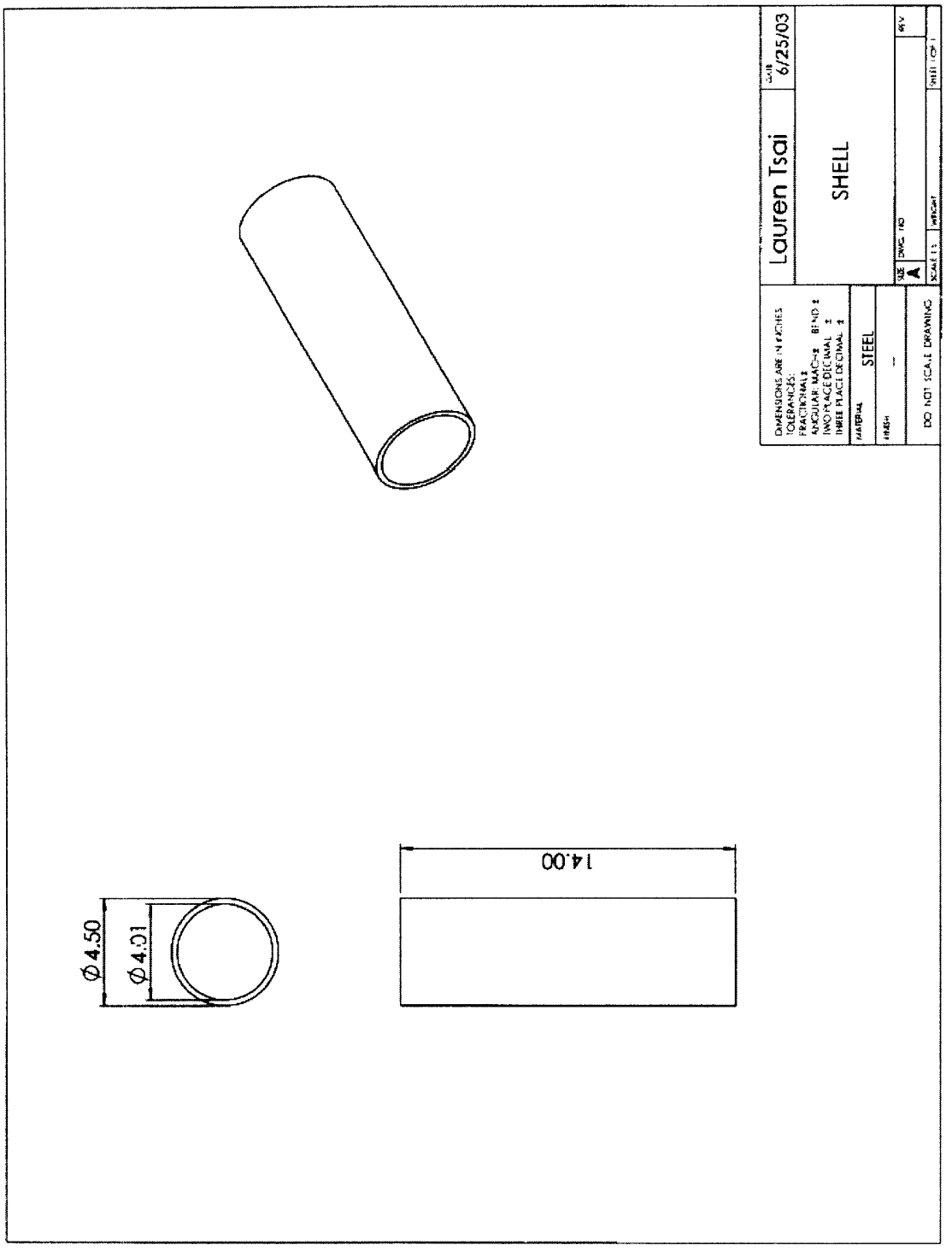

Figure 29: Shell Part Drawing [2]

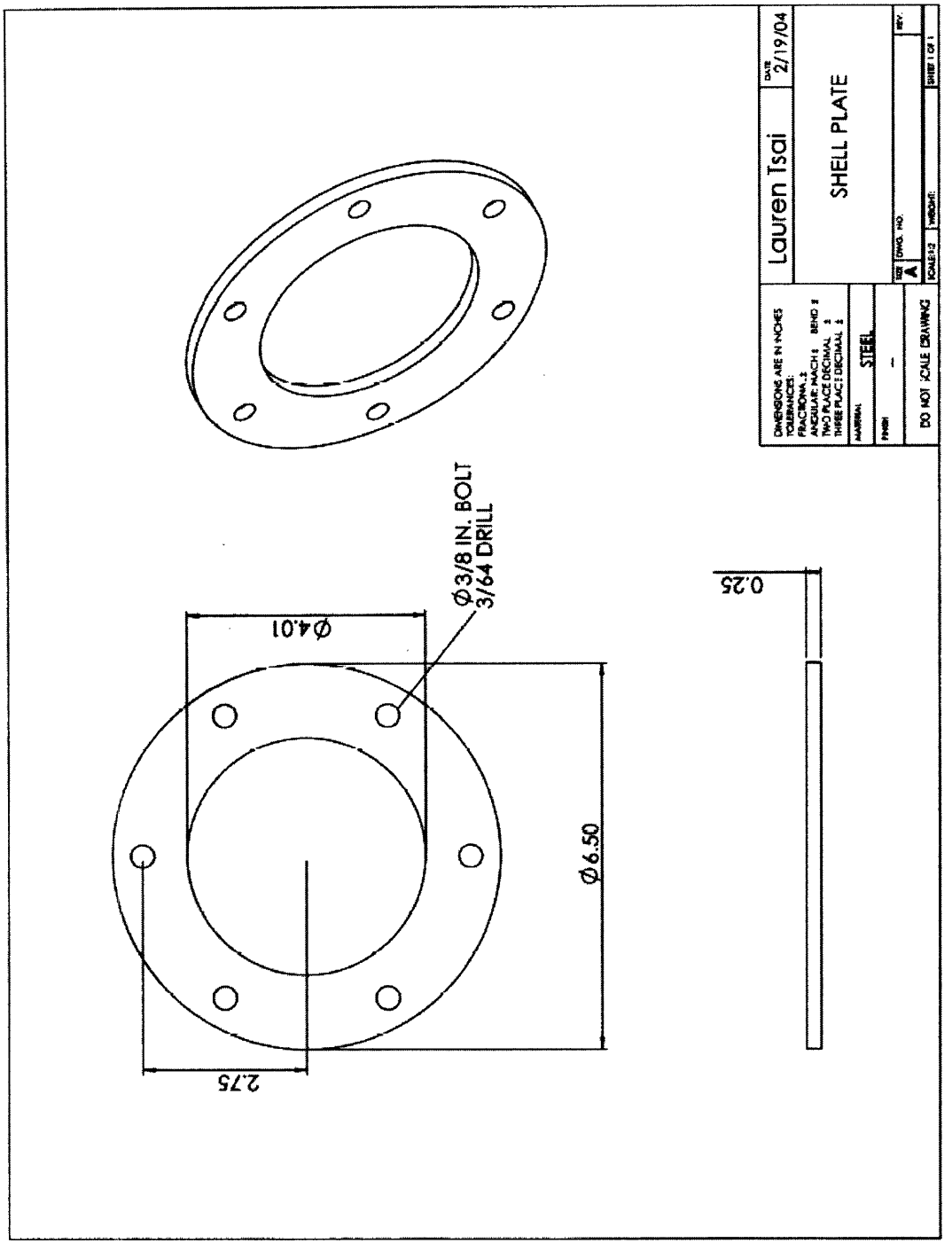

Figure 30: Shell Plate Part Drawing [2]

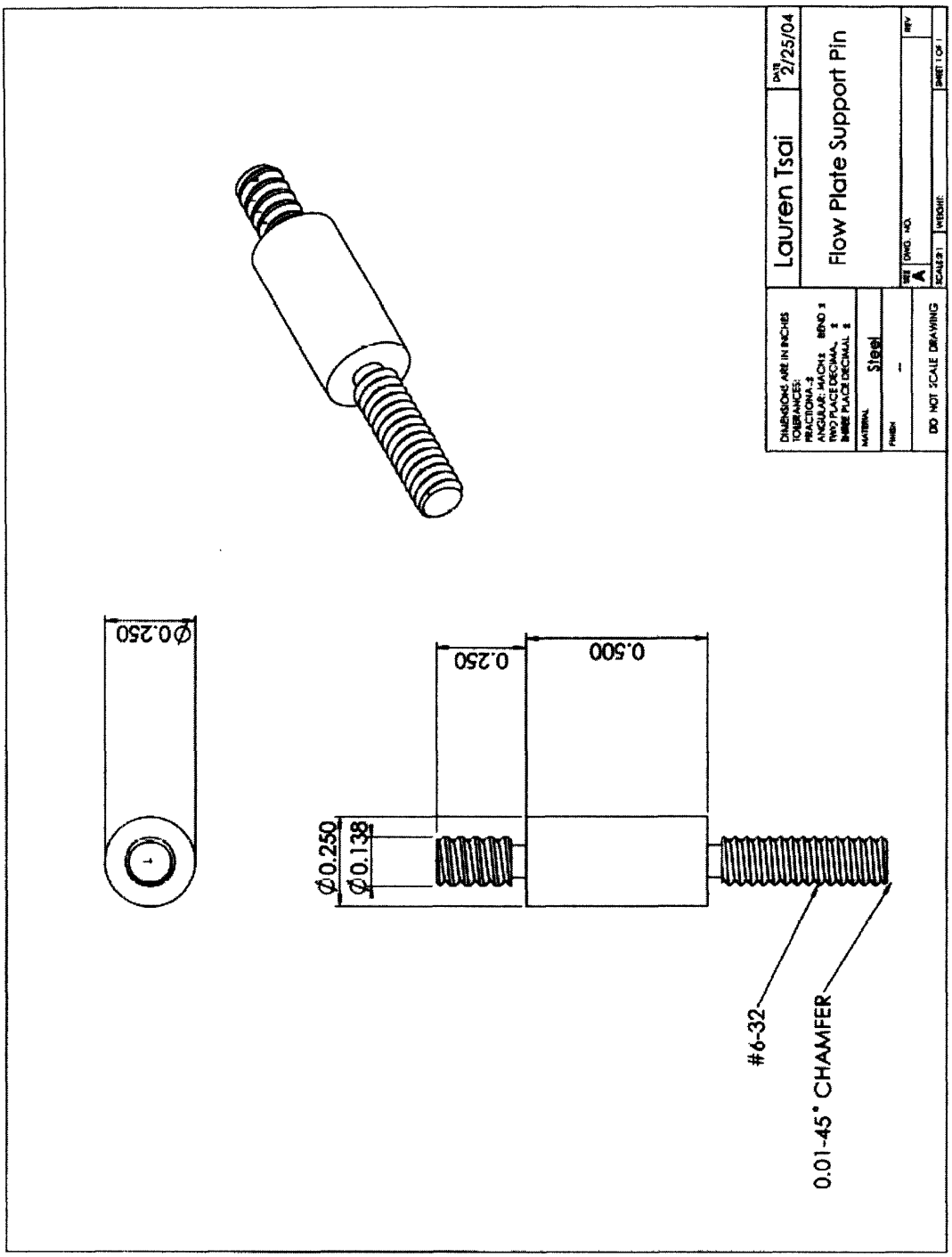

Figure 31: Support Pin Part Drawing [2]

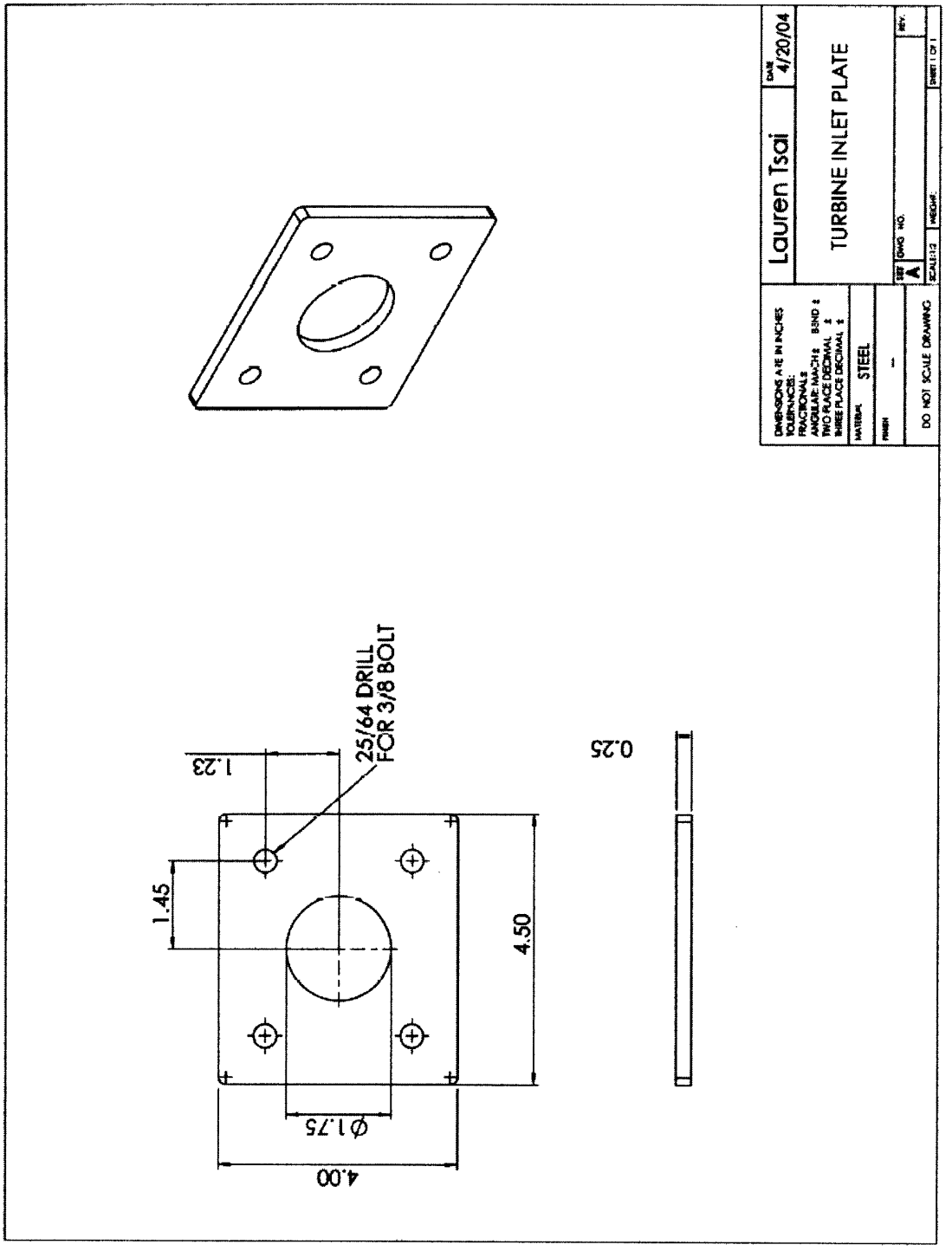

Figure 32: Turbine Inlet Plate Part Drawing [2]

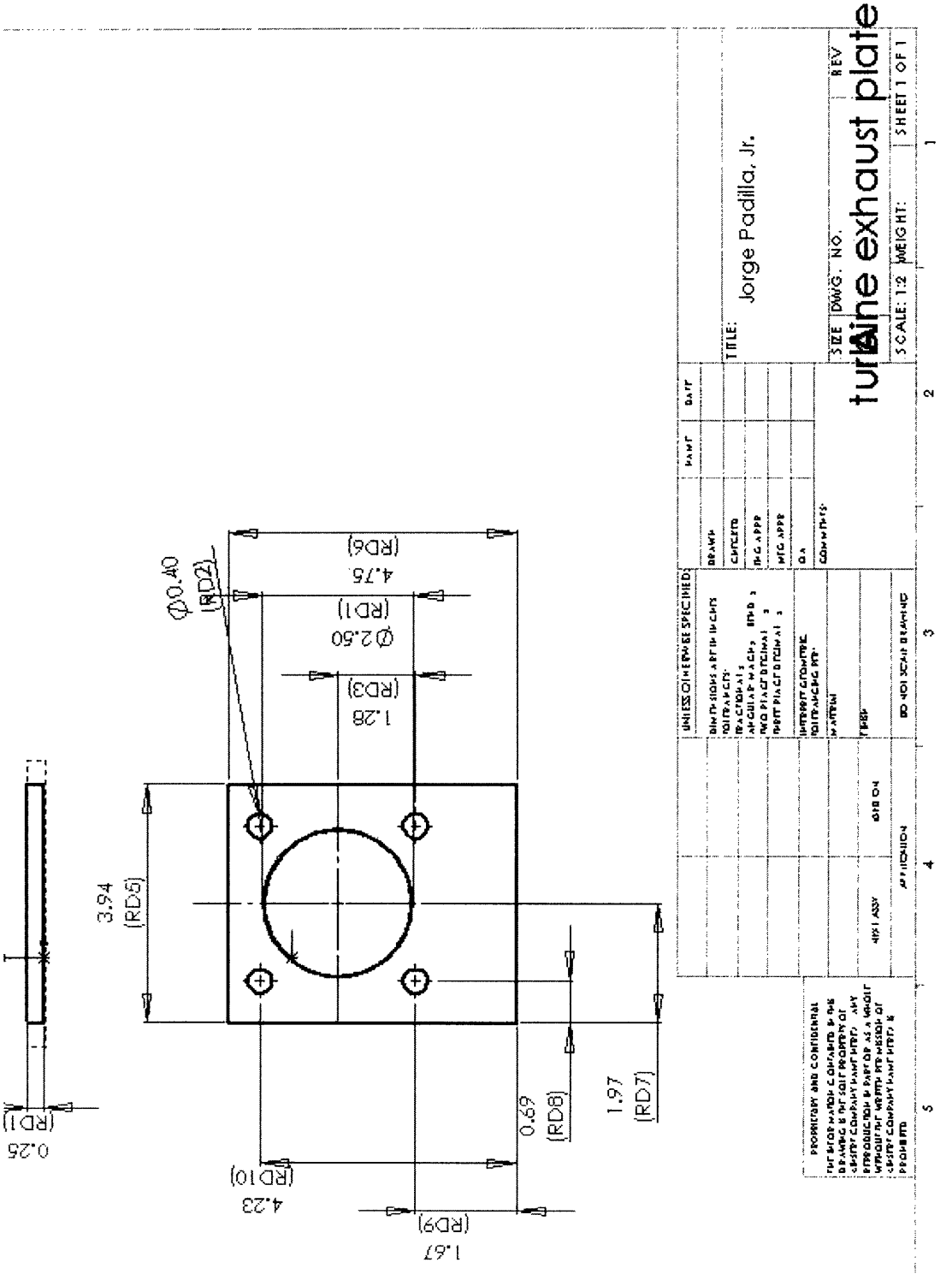

Figure 33: Turbine Exhaust Plate Part Drawing